NBER WORKING PAPER SERIES

THE LUCAS ORCHARD

Ian Martin

Working Paper 17563
http://www.nber.org/papers/w17563

NATIONAL BUREAU OF ECONOMIC RESEARCH
1050 Massachusetts Avenue
Cambridge, MA 02138
November 2011

I thank Tobias Adrian, Malcolm Baker, Thomas Baranga, Robert Barro, John Cochrane, George Constantinides, Josh Coval, Emmanuel Farhi, Xavier Gabaix, Lars Hansen, Jakub Jurek, David Laibson, Robert Lucas, Greg Mankiw, Emi Nakamura, Martin Oehmke, Lubos Pastor, Monika Piazzesi, Roberto Rigobon, David Skeie, Jon Steinsson, Aleh Tsyvinski, Harald Uhlig, Pietro Veronesi, Luis Viceira, James Vickery, and Jiang Wang for their comments. I am particularly grateful to John Campbell and Chris Rogers for their advice. The views expressed herein are those of the author and do not necessarily reflect the views of the National Bureau of Economic Research.

The Lucas Orchard
Ian Martin
NBER Working Paper No. 17563
November 2011
JEL No. G12

ABSTRACT

This paper investigates the behavior of asset prices in an endowment economy in which a representative agent with power utility consumes the dividends of multiple assets. The assets are Lucas trees; a collection of Lucas trees is a Lucas orchard. The model generates return correlations that vary endogenously, spiking at times of disaster. Since disasters spread across assets, the model generates large risk premia even for assets with stable fundamentals. Very small assets may comove endogenously and hence earn positive risk premia even if their fundamentals are independent of the rest of the economy. I provide conditions under which the variation in a small asset's price-dividend ratio can be attributed almost entirely to variation in its risk premium.

Ian Martin
Graduate School of Business
Stanford University
Stanford, CA 94305
and NBER
ian.martin@gsb.stanford.edu

An online appendix is available at:
http://www.nber.org/data-appendix/w17563

This paper investigates the behavior of asset prices in an endowment economy in which a representative agent with power utility consumes the dividends of N assets. The assets are Lucas (1978, 1987) trees, so I call the collection of assets a Lucas orchard. Despite its simple structure, the model generates rich interactions between the prices of assets, including several phenomena that have been documented in the empirical literature; it illustrates "the importance of explicit recognition of the essential interdependences of markets in theoretical and empirical specifications of financial models" (Brainard and Tobin (1968)).

Each of the assets is assumed to have i.i.d. dividend growth over time, though there may be correlation between the dividend growth rates of different assets. This framework allows for the case in which dividends follow geometric Brownian motions, but also allows for a rich structure of jumps in dividends. Standard lognormal models make poor predictions for key asset-pricing quantities such as the equity premium and riskless rate (Mehra and Prescott (1985)). By allowing for rare disasters, I can avoid these puzzles in the manner of Rietz (1988) and Barro (2006), without relying on implausible levels of risk aversion or consumption volatility.

I highlight the important features of the model in a pair of two-tree examples. In the first, dividends follow independent geometric Brownian motions. An asset's valuation ratio depends on its dividend share of consumption: all else equal, an asset is riskier if it contributes a large proportion of consumption than if it contributes a small proportion. A cashflow shock to one asset affects the dividend shares, and hence valuation ratios, of all other assets, so comovement arises even between assets whose dividends are independent. (Such comovement is a feature of the data. Shiller (1989) shows that stock prices in the US and UK move together more closely than do fundamentals, and Forbes and Rigobon (2002) find consistently high levels of interdependence between markets.) In particular, a small asset experiences strong positive comovement in response to good news about a large asset's fundamentals. As a result, the small asset's beta is surprisingly high from a naive point of view, given that its fundamentals are independent of the rest of the market. This behavior was analyzed in the log utility case by Cochrane, Longstaff and Santa-Clara (2008). With log utility, the CAPM holds, so the small asset has a surprisingly high risk premium to go with its surprisingly high beta, but the effects are quantitatively tiny. Things become more interesting as risk aversion rises. Quantitatively, risk premia rise fast, nonlinearly in γ. Qualitatively, the CAPM fails, and the small asset earns a positive alpha. The ICAPM (Merton (1973)) and consumption-CAPM (Breeden (1979)) do hold; here, though, prices are not taken as given but are determined endogenously by exogenous fundamentals.

In the second example, dividends are subject to rare disasters. Now prices, interest rates, and expected returns can jump, so the ICAPM and consumption-CAPM also fail. As noted above, the introduction of disasters enables the model to avoid the equity premium and riskless rate puzzles. Of greater interest, there is an extreme form of comovement: disasters spread across assets. If a large asset experiences a disaster, the price of the other (small) asset drops sharply. This effect provides a new channel through which disasters can contribute to high risk premia. For example, suppose that small asset 1 has perfectly stable dividends, but that large asset 2 is subject to occasional disastrous declines in dividends. Then a disaster for asset 2 leads to a drop in the valuation of asset 1. The possibility of such price drops may induce a substantial risk premium in asset 1, an ostensibly safe asset.

After extending to the general case $N \geq 2$, I revisit these effects in an example with three assets with identical but independent fundamentals ($N = 3$ being the largest case that can be easily represented on paper). With three assets, the state variables are the dividend shares s_1, s_2, and s_3. These add up to one, so the state space can be thought of as the unit simplex. Smaller assets comove positively in response to a positive dividend shock for a large asset, while larger assets comove negatively in response to a positive dividend shock for a small asset. The interplay between these two effects leads to complicated patterns of return correlation at different points in the simplex. Large assets are robustly positively correlated with other assets. Two very small assets are positively correlated with each other, not because they respond positively to each other's shocks—quite the contrary—but because they respond strongly positively to the third, large, asset's shocks. Intermediate between these two cases, small and medium assets have roughly zero return correlation as the two effects—positive comovement with the large asset, negative comovement with each other—cancel out. However, *jumps* isolate the two effects: correlations spike down when a small asset experiences a jump, and spike up when a large asset experiences a jump. These dramatic shifts in correlation do not occur in otherwise similar calibrations without jumps.

Although one might have expected the effects of interest would not be empirically relevant for assets that make up a small share of overall consumption, it is clear from the examples that in fact some of the effects are strongest when an asset is extremely small. To address this issue I consider, in the $N = 2$ case, the limit in which one of the two assets is negligibly small by comparison with the other. This limit represents the most extreme departure from simple models in which price-dividend ratios are constant, and crystallizes some distinctive features of the model. To illustrate this, suppose that the two assets have independent dividend streams. It seems plausible that a small idiosyncratic asset should

earn no risk premium and that it can be valued using a Gordon growth formula, so its dividend yield should equal the riskless rate minus expected dividend growth. I show that this intuition is correct whenever the result of the calculation is meaningful (i.e. positive). But what happens if the riskless rate (determined by the characteristics of the large asset) is less than the mean dividend growth of the small asset? I show that the small asset then has a price-consumption ratio that, as one would expect, tends to zero in the limit; it also a dividend yield of zero in the limit, so its expected return can be attributed entirely to expected capital gains. An unexpected phenomenon emerges: despite its independent fundamentals and negligible size, the small asset comoves endogenously, and hence earns a positive risk premium. In the general case, I provide a precise characterization of when the Gordon growth model does and does not apply, and solve for the limiting riskless rate, risk premium and price-dividend ratio in closed form.

I also derive simple closed-form approximations for these quantities that are valid *near* the small-asset limit. Time variation in the dividend share of the small asset induces time variation in its price-dividend ratio, in its expected excess return, and in the riskless rate. Under certain conditions, variation in the small asset's price-dividend ratio can be attributed to variation in its expected *excess* return: variation in the riskless rate is negligible by comparison. This is a feature of the data emphasized by Cochrane (2005, p. 400). I also show that when the Gordon growth model breaks down for a small asset, its log price-dividend ratio follows an (approximate) random walk.

The same phenomena are present in the example with $N = 3$, though I am not able to derive analytical results. Nonetheless, the intuition for what is going on is the same: if the riskless rate is lower than a very small, idiosyncratic asset's dividend growth rate, then the very small asset has an enormous valuation ratio that is sensitively dependent on news for the large asset.[1] As a result, it comoves and earns a high risk premium.

At one level, it is the interaction between multiplicative structure (power utility and i.i.d. log dividend growth) and additive structure (consumption is the sum of dividends) that makes the model hard to solve. I solve for prices, returns, and interest rates in terms of integral formulas that can be evaluated numerically, subject to conditions that ensure finiteness of asset prices, and hence of the representative agent's expected utility. When there are two assets whose dividends follow geometric Brownian motions, or when one of

[1] In the case where the two other assets are both medium-sized, the riskless rate is high enough that the standard Gordon growth model applies: with more than two assets, both types of behavior can be present in the same calibration, in different regions of the state space.

the two assets is negligibly small, the integrals can be solved in closed form using techniques from complex analysis, notably the residue theorem.

The tractability of the model in the general i.i.d. case is due in part to the use of the cumulant-generating function (CGF). Martin (2008) expresses the riskless rate, risk premium, and consumption-wealth ratio in terms of the CGF in the case $N = 1$, and the expressions found there are echoed here. Working with the CGF, the mathematics is no harder than when working with lognormal models, and there are some important advantages. Most obviously, the model can handle jumps. A second benefit is that CGFs bring a perspective that actually clarifies some of the proofs. If we had restricted to the lognormal special case, it would have seemed natural to prove some of the main results by tedious and unenlightening algebra. Working in more generality, it becomes clear that the same results can be proved more cleanly by exploiting convexity of the CGF. (This is not to claim that no tedious algebra remains.) Finally, the CGF wraps the technological side of the model into a convenient package that simplifies—up to a point—what would otherwise be extremely complicated formulas.

Various authors have investigated multi-asset equilibrium models. Brainard and Tobin (1992, section 8) investigate a two-asset model in which per-period endowments are specified by a Markov chain with a small number of states. They present limited numerical results, and—after noting that their "model is simple and abstract; nevertheless it is not easy to analyze"—no analytical results. Dumas (1992) considers a two-tree production-based model with shipping costs. Menzly, Santos and Veronesi (2004) and Santos and Veronesi (2006) present models in which the dividend shares of assets are assumed to follow mean-reverting processes. By picking convenient functional forms for these processes, closed-form pricing formulas are available, at the cost of complicated interactions between the cashflows of different assets. Pavlova and Rigobon (2007) solve an international asset pricing model, but impose log-linear preferences so price-dividend ratios are constant. The most closely related paper is that of Cochrane, Longstaff and Santa-Clara (2008), who solve the model with log utility, two assets, and dividends following geometric Brownian motions. My solution technique allows for power utility, for jumps in dividends, and for $N \geq 2$ assets. I also solve for bond yields, and hence expand the set of predictions made by the model.

When not included in the main body of the paper, proofs are in the Appendix.

1 Setup

Time is continuous, and runs from 0 (the present) to infinity. There is a representative agent with power utility over consumption C_t, with coefficient of relative risk aversion γ (a positive integer) and time preference rate ρ. The Euler equation, derived by Lucas (1978), prices an asset with dividend stream $\{X_t\}$:

$$P_X = \mathbb{E} \int_0^\infty e^{-\rho t} \left(\frac{C_t}{C_0} \right)^{-\gamma} \cdot X_t \, dt \,. \tag{1}$$

There are N assets, indexed $i = 1, \ldots, N$, that throw off random dividend streams D_{it}. Dividends are positive, which makes it natural to work with log dividends, $y_{it} \equiv \log D_{it}$. At time 0, the dividends $(y_{10}, \ldots, y_{N0})$ of the assets are arbitrary. The vector $\widetilde{\boldsymbol{y}}_t \equiv \boldsymbol{y}_t - \boldsymbol{y}_0 \equiv (y_{1t} - y_{10}, \ldots, y_{Nt} - y_{N0})$ is assumed to follow a Lévy process. This is the continuous-time analogue of the discrete-time assumption that dividend growth is i.i.d.: it allows for the possibility that the assets' dividends grow deterministically, though I assume throughout that at least one of the assets is nondeterministic (the fully deterministic case being trivial). In the special case in which $\widetilde{\boldsymbol{y}}$ is a jump-diffusion, we can write

$$\boldsymbol{y}_t = \boldsymbol{y}_0 + \boldsymbol{\mu} t + \boldsymbol{A}\boldsymbol{Z}_t + \sum_{k=1}^{K(t)} \boldsymbol{J}^k \ . \tag{2}$$

Here $\boldsymbol{\mu}$ is an N-dimensional vector of drifts, $\boldsymbol{A}$ a $N \times N$ matrix of factor loadings, $\boldsymbol{Z}_t$ an N-dimensional Brownian motion, $K(t)$ a Poisson process with arrival rate ω that represents the number of jumps that have taken place by time t, and $\boldsymbol{J}^k$ are N-dimensional i.i.d. random variables. (I will write $\boldsymbol{J} \equiv \boldsymbol{J}^1$ when I discuss the distribution of these random variables.) This framework allows for the possibility that different jumps affect different subsets of the assets. The covariance matrix of the diffusion components of the N dividend processes is $\boldsymbol{\Sigma} \equiv \boldsymbol{A}\boldsymbol{A}'$, whose elements I write as σ_{ij}.

The following definition introduces an object which turns out to capture all relevant information about the stochastic processes driving dividend growth.

Definition 1. *The* cumulant-generating function $\boldsymbol{c}(\boldsymbol{\theta})$ *is defined for* $\boldsymbol{\theta} \in \mathbb{R}^N$ *by*

$$\boldsymbol{c}(\boldsymbol{\theta}) \equiv \log \mathbb{E} \exp \boldsymbol{\theta}' (\widetilde{\boldsymbol{y}}_{t+1} - \widetilde{\boldsymbol{y}}_t).$$

Since Lévy processes have i.i.d. increments, $\boldsymbol{c}(\boldsymbol{\theta})$ is independent of t. Table 1, below, provides conditions that ensure that asset prices are finite. In general, the CGF takes the

form given in the Lévy-Khintchine representation. If log dividends follow a jump-diffusion as in (2), then $\boldsymbol{c}(\boldsymbol{\theta}) = \boldsymbol{\theta}'\boldsymbol{\mu} + \boldsymbol{\theta}'\boldsymbol{\Sigma}\boldsymbol{\theta}/2 + \omega\left(\mathbb{E}\, e^{\boldsymbol{\theta}'\boldsymbol{J}} - 1\right)$.

I close the model by assuming that the representative investor holds the market, and that dividends are not storable, so that $C_t = D_{1t} + \cdots + D_{Nt}$.

2 The two-asset case

2.1 A suggestive example

Consider the problem of pricing the claim to asset 1's output with log utility. We have

$$\begin{aligned} P_{10} &= \mathbb{E}\int_0^\infty e^{-\rho t}\left(\frac{C_t}{C_0}\right)^{-1}\cdot D_{1t}\,dt \\ &= (D_{10}+D_{20})\int_0^\infty e^{-\rho t}\,\mathbb{E}\left(\frac{D_{1t}}{D_{1t}+D_{2t}}\right)dt\,, \end{aligned}$$

and unfortunately this expectation is not easy to calculate. This, essentially, is the major analytical challenge confronted by Cochrane, Longstaff and Santa-Clara (2008).

Here, though, is an instructive case in which the expectation simplifies considerably. Suppose that $D_{1t} < 1$ and $D_{2t} \equiv 1$ at all times t, so that asset 2 is safe, but asset 1 is subject to downward jumps at random times. (The jumps may be random in size, but they must always be downwards.) Then we can expand the expectation as a geometric sum:

$$\mathbb{E}\left(\frac{D_{1t}}{1+D_{1t}}\right) = \mathbb{E}\left[D_{1t} - D_{1t}^2 + D_{1t}^3 - \ldots\right] = \sum_{n=1}^{\infty}(-1)^{n+1}D_{10}^n e^{\boldsymbol{c}(n,0)t}\,.$$

Substituting back, we find that

$$P_{10} = (1+D_{10})\int_{t=0}^\infty e^{-\rho t}\sum_{n=1}^{\infty}(-1)^{n+1}D_{10}^n e^{\boldsymbol{c}(n,0)t} = (1+D_{10})\sum_{n=1}^{\infty}\frac{(-1)^{n+1}D_{10}^n}{\rho - \boldsymbol{c}(n,0)}\,.$$

If we define $s \equiv D_{10}/(D_{10}+D_{20})$ to be the share of asset 1 in global output—a definition which is maintained throughout—we can rewrite this as

$$P_{10}/D_{10} = \frac{1}{\sqrt{s(1-s)}}\sum_{n=0}^{\infty}\frac{(-1)^n(\frac{s}{1-s})^{n+1/2}}{\rho - \boldsymbol{c}(n+1,0)}. \tag{3}$$

This expression is easy to evaluate numerically once asset 1's dividend process—and hence $\boldsymbol{c}(\theta,0)$—is specified. For example, if asset 1's log dividend is subject to downward jumps of constant size $-b$ arriving at rate ω, then $\boldsymbol{c}(\theta,0) = \omega(e^{-b\theta}-1)$, so $\rho - \boldsymbol{c}(n+1,0) \to \rho+\omega$ as $n\to\infty$. Meanwhile, $s/(1-s) < 1$ so the terms in the numerator of the summand decline at geometric rate and numerical summation will converge fast.

In this special example, we can write $D_{1t}/(1+D_{1t})$ as a geometric sum. In the general case, the analogous move is to write the equivalent of $D_{1t}/(1+D_{1t})$ as a Fourier integral before computing the expectation. The gain from doing so is that, as above, it converts the otherwise intractable function inside the expectation into an expression involving powers of terms in D_{1t} and D_{2t}, which can be dealt with using the CGF.

2.2 The general solution

Consider an asset with dividend stream $D_{\boldsymbol{\alpha},t} \equiv D_{1t}^{\alpha_1} D_{2t}^{\alpha_2}$, $\boldsymbol{\alpha} \equiv (\alpha_1, \alpha_2) \in \{(1,0),(0,1),(0,0)\}$. The three alternatives represent asset 1, asset 2, and a riskless perpetuity respectively. Asset prices depend on the value of $s_t = D_{1t}/(D_{1t}+D_{2t}) \in [0,1]$, the share of aggregate consumption contributed by the dividend of asset 1. It is often more convenient to use a state variable that is a monotonic transformation of s:

$$u_t = \log\left(\frac{1-s_t}{s_t}\right) = y_{2t} - y_{1t}.$$

While s_t ranges between 0 and 1, u_t takes values between $-\infty$ and $+\infty$. As asset 1 becomes small, u_t tends to infinity; as asset 1 becomes large, u_t tends to minus infinity. Since y_{1t} and y_{2t} follow Lévy processes, u_t does too. If, say, dividends follow geometric Brownian motions with equal mean log dividend growth, then u_t is a driftless Brownian motion.

The next result supplies an integral formula for the price-dividend ratio on the $\boldsymbol{\alpha}$-asset. In the formula, i represents $\sqrt{-1}$. From now on, I drop the subscript t on state variables.

Proposition 1 (The pricing formula)**.** *The price-dividend ratio on an asset with dividend share s that pays dividend stream $D_{\boldsymbol{\alpha},t} \equiv D_{1t}^{\alpha_1} D_{2t}^{\alpha_2}$ is*

$$\frac{P_{\boldsymbol{\alpha}}}{D_{\boldsymbol{\alpha}}}(u) = [2\cosh(u/2)]^{\gamma} \cdot \int_{-\infty}^{\infty} \frac{e^{iuz}\mathscr{F}_{\gamma}(z)}{\rho - \boldsymbol{c}(\alpha_1 - \gamma/2 - iz, \alpha_2 - \gamma/2 + iz)}\, dz\,, \tag{4}$$

where

$$\mathscr{F}_{\gamma}(z) \equiv \frac{1}{2\pi} \cdot \frac{\Gamma(\gamma/2+iz)\Gamma(\gamma/2-iz)}{\Gamma(\gamma)}\,. \tag{5}$$

Proof. The price of the $\boldsymbol{\alpha}$-asset is

$$\begin{aligned} P_{\boldsymbol{\alpha}} &= \mathbb{E}\int_0^{\infty} e^{-\rho t}\left(\frac{C_t}{C_0}\right)^{-\gamma} D_{1t}^{\alpha_1} D_{2t}^{\alpha_2}\, dt \\ &= (C_0)^{\gamma}\int_0^{\infty} e^{-\rho t}\,\mathbb{E}\left(\frac{e^{\alpha_1(y_{10}+\widetilde{y}_{1t})+\alpha_2(y_{20}+\widetilde{y}_{2t})}}{\left[e^{y_{10}+\widetilde{y}_{1t}}+e^{y_{20}+\widetilde{y}_{2t}}\right]^{\gamma}}\right) dt\,. \end{aligned}$$

It follows that

$$\frac{P_{\boldsymbol{\alpha}}}{D_{\boldsymbol{\alpha}}} = (e^{y_{10}} + e^{y_{20}})^{\gamma} \int_{t=0}^{\infty} e^{-\rho t}\, \mathbb{E}\left(\frac{e^{\alpha_1 \widetilde{y}_{1t} + \alpha_2 \widetilde{y}_{2t}}}{\left[e^{y_{10}+\widetilde{y}_{1t}} + e^{y_{20}+\widetilde{y}_{2t}}\right]^{\gamma}} \right) dt\,.$$

The expectation inside the integral is calculated, via a Fourier transform, in equation (24) of Appendix A.1. Interchanging the order of integration—since the integrand is absolutely integrable, Fubini's theorem applies—and writing u for $y_{20} - y_{10}$, we obtain (4):

$$\begin{aligned} \frac{P_{\boldsymbol{\alpha}}}{D_{\boldsymbol{\alpha}}} &= [2\cosh(u/2)]^{\gamma} \int_{z=-\infty}^{\infty} \int_{t=0}^{\infty} e^{-\rho t} e^{\boldsymbol{c}(\alpha_1 - \gamma/2 - iz, \alpha_2 - \gamma/2 + iz)t} \cdot e^{iuv} \mathscr{F}_{\gamma}(z)\, dt\, dz \\ &\overset{(a)}{=} [2\cosh(u/2)]^{\gamma} \int_{z=-\infty}^{\infty} \frac{e^{iuz} \mathscr{F}_{\gamma}(z)}{\rho - \boldsymbol{c}(\alpha_1 - \gamma/2 - iz, \alpha_2 - \gamma/2 + iz)}\, dz. \end{aligned}$$

Equality (a) is valid if $\rho - \mathrm{Re}[\boldsymbol{c}(\alpha_1 - \gamma/2 - iz, \alpha_2 - \gamma/2 + iz)] > 0$ for all $z \in \mathbb{R}$. In Appendix A.3, I show that this inequality holds for all $z \in \mathbb{R}$ if it holds at $z = 0$, i.e. so long as $\rho - \boldsymbol{c}(\alpha_1 - \gamma/2, \alpha_2 - \gamma/2) > 0$. I refer to this as the finiteness condition, and assume that it holds when $(\alpha_1, \alpha_2) = (1, 0)$, $(0, 1)$, or $(0, 0)$. □

The pricing formula (4) allows for the stochastic process governing log outputs to be any Lévy process satisfying the assumptions of Table 1. Moreover, $\mathscr{F}_{\gamma}(z)$ is a strictly positive function which is symmetric about $z = 0$, where it attains its maximum, and decays exponentially fast towards zero as $|z| \to \infty$, so (4) can easily be evaluated numerically. Equation (25) of the Appendix provides an alternative representation of $\mathscr{F}_{\gamma}(z)$ in terms of elementary functions, though it is less compact than (5).

The proof of Proposition 1 shows that for $s \in (0, 1)$, finiteness of the prices of the two assets—and hence of expected utility—is assured by the assumptions that $\rho - \boldsymbol{c}(1 - \gamma/2, -\gamma/2) > 0$ and $\rho - \boldsymbol{c}(-\gamma/2, 1 - \gamma/2) > 0$. I also assume that $\rho - \boldsymbol{c}(1 - \gamma, 0) > 0$ and $\rho - \boldsymbol{c}(0, 1 - \gamma) > 0$, so that aggregate wealth is finite at the limit points $s = 0$ and $s = 1$.

Restriction	Reason
$\rho - \boldsymbol{c}(1 - \gamma/2, -\gamma/2) > 0$	finite price of asset 1
$\rho - \boldsymbol{c}(-\gamma/2, 1 - \gamma/2) > 0$	finite price of asset 2
$\rho - \boldsymbol{c}(1 - \gamma, 0) > 0$	finite aggregate wealth in limit $s \to 1$
$\rho - \boldsymbol{c}(0, 1 - \gamma) > 0$	finite aggregate wealth in limit $s \to 0$

Table 1: The restrictions imposed on the model.

For many practical purposes, this is the end of the story, since the integral formula is

very well behaved and can be calculated numerically almost instantly; I take this direct route in Section 2.3. But the pen-and-paper approach can be pushed further in some cases.

To explain how, we need some terminology. Let f be a complex-valued function. The function f is *holomorphic* in a subset G of the complex plane if $\lim_{h\to 0}[f(z+h)-f(z)]/h$ exists for all z in some open set containing G. To give some examples, polynomials, convergent power series, the exponential function, sine and cosine are holomorphic; and compositions and finite sums and products of holomorphic functions are holomorphic.[2]

Complex integration takes place over paths in the complex plane: an integral might be "along the real axis from $-\infty$ to $+\infty$"; "around the unit circle $|z| = 1$"; or "along the real line from $-R$ to R, then around a semicircular arc lying in the upper half-plane from R back to $-R$." Integrals like (4) have integrands that are holomorphic everywhere except at certain *singularities*, away from the path of integration, where they explode to infinity. If f is holomorphic in some punctured disc $D'(a;r) \equiv \{z \in \mathbb{C} : 0 < |z-a| < r\}$, but not at a, then a is an *isolated singularity*: for example, $f(z) = 1/z$ is holomorphic except for at an isolated singularity at the origin. In this case, f has a unique power series expansion $f(z) = \sum_{n=-\infty}^{\infty} c_n(z-a)^n$ for $z \in D'(a;r)$. If $c_n = 0$ for all $n < 0$, the point a is a *removable singularity*. (In other words, it is not "really" a singularity at all. Consider $f(z) = \sin z/z$, whose singularity at 0 can be removed by defining $f(0) = 1$.) If there is some positive m such that $c_{-m} \neq 0$ and $c_k = 0$ for all $k < -m$ then the point a is a *pole (of order m)*. The *residue* of f at a, written $\operatorname{Res}\{f(z);a\}$, is defined to be the coefficient on the term $(z-a)^{-1}$ in a power series expansion of $f(z)$. If $f(z) = g(z)/h(z)$, where $g(a) \neq 0$, $h(a) = 0$, and $h'(a) \neq 0$, so that $f(z)$ has a pole at a, then $\operatorname{Res}\{f(z);a\} = g(a)/h'(a)$: I use this repeatedly in Appendices A.4 and A.5. The result that makes all this so useful is

Fact 1 (The residue theorem)**.** *Let Ω denote a closed path of integration which is to be integrated around in an anticlockwise direction. If f is holomorphic inside and on Ω, except for at a finite number of poles at points $a_1, \ldots, a_m$ inside Ω, then*

$$\int_\Omega f(z)\,dz = 2\pi i \sum_{j=1}^{m} \operatorname{Res}\{f(z);a_j\}.$$

It is an amazing—and powerful—fact that such an integral can be computed by analyzing the behavior of the integrand at its poles. To illustrate, I show how to derive (3)

[2]Evidently, to be holomorphic is to be complex-differentiable. But note that not every function that is differentiable when considered as a function from $\mathbb{R}^2 \to \mathbb{R}^2$ is differentiable when considered as a function from $\mathbb{C} \to \mathbb{C}$. For example, complex conjugation, which maps $x + iy \mapsto x - iy$, is not holomorphic, although the function from $\mathbb{R}^2$ to $\mathbb{R}^2$ that maps $(x, y) \mapsto (x, -y)$ is differentiable.

from the more general (4). Doing so also provides a roadmap for the Brownian motion case that will be considered below. To streamline the discussion I proceed heuristically, taking as given various facts that are proved for the Brownian motion case in Appendix A.4.

The expression (3) is valid for $s < 1/2$, i.e. $u > 0$. Setting $\gamma = 1$ in (4), substituting $\alpha_1 = 1, \alpha_2 = 0$ to calculate the price-dividend ratio of asset 1, and imposing the fact that $D_{2t} \equiv 1$, so that $\boldsymbol{c}(\theta_1, \theta_2)$ is independent of θ_2 and equals, say, $\boldsymbol{c}(\theta_1, 0)$, we get

$$P_{10}/D_{10} = [2\cosh(u/2)] \cdot \int_{-\infty}^{\infty} \frac{e^{iuz}\mathscr{F}_1(z)}{\rho - \boldsymbol{c}(1/2 - iz, 0)}\, dz\,. \tag{6}$$

We now proceed in a series of steps. The basic strategy is to attack (6) via the residue theorem. To do so, we must integrate around a closed contour, rather than over the real axis. Loosely speaking, we want to integrate from $-\infty$ to $+\infty$ and then loop back along the arc of an infinitely large semicircle. More formally, we will consider the limit of a sequence of integrals around increasingly large semicircles with bases lying along the real axis. Each of these integrals can be evaluated using the residue theorem, by summing over residues inside these increasingly large semicircles. In the limit, the contribution of the integral along the semicircular arc—as opposed to the base—tends to zero. (This often happens with integrals that are amenable to this line of attack.) The upshot is that the original integral (6) equals $2\pi i$ times the sum of *all* the residues of the integrand $e^{iuz}\mathscr{F}_1(z)/[\rho - \boldsymbol{c}(1/2 - iz, 0)]$ in the upper half plane. These residues occur at the poles of this function, i.e. at the poles of $\mathscr{F}_1(z)$ and at the zeros of $\rho - \boldsymbol{c}(1/2 - iz, 0)$.

In this example, things are particularly simple because there are no zeros of $\rho - \boldsymbol{c}(1/2 - iz, 0)$ for z in the upper half-plane.[3] It remains to consider the poles of $\mathscr{F}_1(z) = (1/2\pi)\Gamma(1/2 + iz)\Gamma(1/2 - iz)$. We will need two standard properties of the Γ-function. First, $\Gamma(n) = (n-1)!$ for positive integer n. Second, $\Gamma(z)$ has poles only at zero and at the negative real integers, and the residue at $-n$ is $(-1)^n/n!$. As a result, the poles of $e^{iuz}\mathscr{F}_1(z)/[\rho - \boldsymbol{c}(1/2 - iz, 0)]$ occur at $z = (n + 1/2)i$ for $n = 0, 1, 2, \ldots$, and the residue at $(n + 1/2)i$ is

$$\frac{e^{-(n+1/2)u}(-1)^n\Gamma(n+1)/n!}{2\pi i \cdot [\rho - \boldsymbol{c}(n+1, 0)]} = \frac{(-1)^n(\frac{s}{1-s})^{n+1/2}}{2\pi i \cdot [\rho - \boldsymbol{c}(n+1, 0)]}\,.$$

Summing over all the residues, $n = 0, 1, \ldots$, multiplying by $2\pi i$, and rearranging,

$$P/D(s) = \frac{1}{\sqrt{s(1-s)}} \sum_{n=0}^{\infty} \frac{(-1)^n(\frac{s}{1-s})^{n+1/2}}{\rho - \boldsymbol{c}(n+1, 0)}\,,$$

[3] By the finiteness condition, $\rho - \boldsymbol{c}(1/2, -1/2) = \rho - \boldsymbol{c}(1/2, 0) > 0$. Moreover, $\boldsymbol{c}(x, 0)$ is decreasing in x since $D_{1t} < 1$, so $\rho - \boldsymbol{c}(1/2 + k, 0) > 0$ for all $k > 0$. It follows from Lemma 1 of Appendix A.3 that $\mathrm{Re}\,[\rho - \boldsymbol{c}(1/2 - iz, 0)] \geq \rho - \boldsymbol{c}(\mathrm{Re}(1/2 - iz), 0) = \rho - \boldsymbol{c}(1/2 + \mathrm{Im}\, z, 0) > 0$ for all z in the upper half-plane.

as in equation (3). This example illustrates the more general point that residues at two types of poles contribute to the integral: (i) poles of $\mathscr{F}_\gamma(z)$, which are located at regularly spaced points $(n+\gamma/2)i$, for $n = 0, 1, 2, \ldots$, on the imaginary axis; and (ii) poles of $1/\left[\rho - \boldsymbol{c}(1-\gamma/2-iz, -\gamma/2+iz)\right]$. The Brownian motion case is tractable because $\boldsymbol{c}(\theta_1, \theta_2)$ is quadratic in θ_1 and θ_2, so the latter poles occur at zeros of the quadratic $\rho - \boldsymbol{c}(1-\gamma/2-iz, -\gamma/2+iz)$, of which there is exactly one in the upper half-plane.

Now we return to the general case. The expected return on an asset paying dividend stream $D_{\boldsymbol{\alpha},t}$ can be expressed in terms of integrals very similar to those that appear in the general price-dividend formula. The instantaneous expected return, $R_{\boldsymbol{\alpha}}$, is defined by

$$R_{\boldsymbol{\alpha}} dt \equiv \underbrace{\frac{\mathbb{E}\, dP_{\boldsymbol{\alpha}}}{P_{\boldsymbol{\alpha}}}}_{\text{capital gains}} + \underbrace{\frac{D_{\boldsymbol{\alpha}}}{P_{\boldsymbol{\alpha}}} dt}_{\text{dividend yield}} .$$

Proposition 2 (Expected returns)**.** *If γ is a positive integer, then $R_{\boldsymbol{\alpha}}$ is given by*

$$R_{\boldsymbol{\alpha}}(u) = \frac{\displaystyle\sum_{m=0}^{\gamma} \binom{\gamma}{m} e^{-mu} \int_{-\infty}^{\infty} h(z) e^{iuz} \cdot \boldsymbol{c}(\boldsymbol{w}_m(z))\, dz}{\displaystyle\sum_{m=0}^{\gamma} \binom{\gamma}{m} e^{-mu} \int_{-\infty}^{\infty} h(z) e^{iuz}\, dz} + \frac{D_{\boldsymbol{\alpha}}}{P_{\boldsymbol{\alpha}}}(u) \tag{7}$$

where $h(z) \equiv \mathscr{F}_\gamma(z)/[\rho - \boldsymbol{c}(\alpha_1 - \gamma/2 - iz, \alpha_2 - \gamma/2 + iz)]$ and $\boldsymbol{w}_m(z) \equiv (\alpha_1 - \gamma/2 + m - iz, \alpha_2 + \gamma/2 - m + iz)$.

Write B_T for the time-0 price of a zero-coupon bond which pays one unit of the consumption good at time T, and define the yield to time T, $\mathscr{Y}(T)$, by $B_T = e^{-\mathscr{Y}(T)\cdot T}$, and the instantaneous riskless rate to be $r \equiv \lim_{T \downarrow 0} \mathscr{Y}(T)$. The next result expresses interest rates in terms of the state variable u. The framework can generate upward- or downward-sloping yield curves and humped curves with an inverse-U shape.

Proposition 3 (Real interest rates)**.** *The yield to time T is*

$$\mathscr{Y}(T) = -\frac{1}{T} \log \left\{ [2\cosh(u/2)]^\gamma \int_{-\infty}^{\infty} \mathscr{F}_\gamma(v) e^{iuz} \cdot e^{-[\rho - \boldsymbol{c}(-\gamma/2 - iz, -\gamma/2 + iz)]T}\, dz \right\} . \tag{8}$$

The instantaneous riskless rate is

$$r = [2\cosh(u/2)]^\gamma \int_{-\infty}^{\infty} \mathscr{F}_\gamma(z) e^{iuz} \cdot \left[\rho - \boldsymbol{c}(-\gamma/2 - iz, -\gamma/2 + iz)\right]\, dz\,. \tag{9}$$

The long rate is a constant, independent of the current state u, given by

$$\lim_{T \to \infty} \mathscr{Y}(T) = \max_{\theta \in [-\gamma/2, \gamma/2]} \rho - \boldsymbol{c}(-\gamma/2 + \theta, -\gamma/2 - \theta). \tag{10}$$

In a symmetric calibration, $\lim_{T\to\infty} \mathscr{Y}(T) = \rho - \boldsymbol{c}(-\gamma/2, -\gamma/2)$.

For comparison, in a one-tree economy with all consumption drawn from tree 1, the yield curve would be flat, with an interest rate of $\rho - \boldsymbol{c}(-\gamma, 0)$; and if all consumption were drawn from tree 2, the interest rate would be $\rho - \boldsymbol{c}(0, -\gamma)$. Equation (10) shows that the long rate is at least as high in the two-tree economy as in either one-tree economy. The long rate is *equal* to the long rate in one of these economies if the requirement in (10) that $\theta \in [-\gamma/2, \gamma/2]$ is binding. In the lognormal case $\boldsymbol{c}(\theta_1, \theta_2) = \mu_1\theta_1 + \mu_2\theta_2 + \frac{1}{2}\sigma_{11}\theta_1^2 + \sigma_{12}\theta_1\theta_2 + \frac{1}{2}\sigma_{22}\theta_2^2$, so $\theta = \gamma/2$, say, occurs if $\mu_1 - \gamma\sigma_{12} \leq \mu_2 - \gamma\sigma_{22}$. This is intuitive: if asset 1's mean dividend growth μ_1 is sufficiently small, then it will be negligible in the distant future, so the long rate $\rho - \boldsymbol{c}(0, -\gamma)$ is determined entirely by the characteristics of asset 2.

It is possible, though, for asset 1 to influence long interest rates even if its share converges to zero over time with probability one. Suppose that $\sigma_{12} = 0$ and $\mu_2 - \gamma\sigma_{22} < \mu_1 < \mu_2$. Then, even though tree 2 dominates in the long run (because $\mu_2 > \mu_1$), the long rate does not equal the rate that would prevail in a tree-2 economy (because $\mu_1 - \gamma\sigma_{12} > \mu_2 - \gamma\sigma_{22}$). This is an instance of a general principle that the pricing of long-dated bonds is very sensitive to bad states of the world (Weitzman (1998), Gollier (2002), Martin (2009))—in this example, to states in which the slow-growing tree makes a significant contribution to consumption.

2.2.1 The Brownian motion case

Suppose now that the dividend processes follow potentially correlated geometric Brownian motions, $dy_i = \mu_i\, dt + \sqrt{\sigma_{ii}}\, dz_i$, $i = 1, 2$. Then asset prices can be expressed in terms of the hypergeometric function $F(a, b; c; z)$, which is defined for $|z| < 1$ by the power series

$$F(a, b; c; z) = 1 + \frac{a \cdot b}{1! \cdot c} z + \frac{a(a+1) \cdot b(b+1)}{2! \cdot c(c+1)} z^2 + \frac{a(a+1)(a+2) \cdot b(b+1)(b+2)}{3! \cdot c(c+1)(c+2)} z^3 + \cdots, \tag{11}$$

and for $|z| \geq 1$ by analytic continuation of this series with respect to z.

Proposition 4 (The Brownian motion case)**.** *When dividends follow geometric Brownian motions and γ is an integer, the price-dividend ratio of the $\boldsymbol{\alpha}$-asset is*

$$\begin{aligned} P/D_1(s) \;=\; & \frac{1}{B(\lambda_1 - \lambda_2)} \left[\frac{1}{(\gamma/2 + \lambda_1)\, s^\gamma}\; F\left(\gamma, \gamma/2 + \lambda_1; 1 + \gamma/2 + \lambda_1; \frac{s-1}{s}\right) + \right. \\ & \left. + \frac{1}{(\gamma/2 - \lambda_2)\,(1-s)^\gamma}\; F\left(\gamma, \gamma/2 - \lambda_2; 1 + \gamma/2 - \lambda_2; \frac{s}{s-1}\right) \right], \end{aligned} \tag{12}$$

where $B \equiv \frac{1}{2}X^2$, $\lambda_1 \equiv \frac{\sqrt{Y^2+X^2Z^2}-Y}{X^2}$, *and* $\lambda_2 \equiv -\frac{\sqrt{Y^2+X^2Z^2}+Y}{X^2}$, *with*

$$\begin{aligned} X^2 &\equiv \sigma_{11} - 2\sigma_{12} + \sigma_{22} \\ Y &\equiv \mu_1 - \mu_2 + \alpha_1(\sigma_{11} - \sigma_{12}) - \alpha_2(\sigma_{22} - \sigma_{12}) - \frac{\gamma}{2}(\sigma_{11} - \sigma_{22}) \\ Z^2 &\equiv 2(\rho - \alpha_1\mu_1 - \alpha_2\mu_2) - (\alpha_1^2\sigma_{11} + 2\alpha_1\alpha_2\sigma_{12} + \alpha_2^2\sigma_{22}) + \\ &\quad + \gamma\left[\mu_1 + \mu_2 + \alpha_1\sigma_{11} + (\alpha_1+\alpha_2)\sigma_{12} + \alpha_2\sigma_{22}\right] - \frac{\gamma^2}{4}(\sigma_{11} + 2\sigma_{12} + \sigma_{22}). \end{aligned}$$

As the notation suggests, X^2 *and* Z^2 *are strictly positive.*

The instantaneous riskless rate is given by

$$\begin{aligned} r &= \rho + \gamma\left[s\left(\mu_1 + \frac{\sigma_{11}}{2}\right) + (1-s)\left(\mu_2 + \frac{\sigma_{22}}{2}\right)\right] - \\ &\quad - \frac{\gamma(\gamma+1)}{2}\left[s^2\sigma_{11} + 2s(1-s)\sigma_{12} + (1-s)^2\sigma_{22}\right]. \end{aligned} \tag{13}$$

Sketch proof. The result follows via the strategy laid out above: the integral formula (4) is equal to the limit of a sequence of contour integrals around increasingly large semicircles in the upper half of the complex plane. By the residue theorem, this limit can be evaluated by summing all residues of the integrand in (4) in the upper half-plane. Carrying out this summation involves some tedious calculation, but we end up at (12).

Appendix A.4 has the details, but Figure 1 illustrates the approach by showing one of the integrals in the sequence for a particular calibration and $u > 0$. The surface is the real

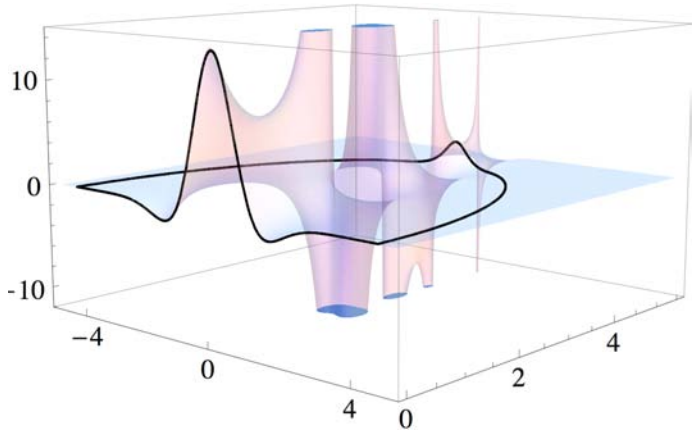

Figure 1: A member of the sequence of contour integrals whose limit is (12).

part of the integrand in (4); several poles are visible where it explodes to infinity. The dark line indicates the semicircular contour along which we integrate, whose base lies on the real axis. By the residue theorem, the integral over the contour can be evaluated by computing

the residues at those poles that happen to lie inside the semicircle. As the semicircle's radius becomes larger and larger, the integral along the base approaches (4), while the integral around the semicircular arc tends to zero. Notice how the arc of the semicircle threads between the poles that form a spine running up the imaginary axis: this is always possible because once we get sufficiently far up the imaginary axis, the poles are evenly spaced.

Finally, the riskless rate r is given, in the Brownian motion case, by $r\,dt = -\mathbb{E}(dM/M)$, where $M_t \equiv e^{-\rho t}C_t^{-\gamma}$; (13) follows by Itô's lemma. □

This result can be extended to the case in which log dividends follow a jump-diffusion as in (2), so long as the only type of jumps that occur are *global jumps*:

Definition 2 (Global jumps)**.** *A jump is* global *if it causes each asset's dividend to decline by the same proportion, i.e.* $J_1^k = J_2^k$ *for all* k *in* (2)*.*

Proposition 5. *If all jumps are global, then equation* (12) *of Proposition 4 continues to hold with* ρ *replaced by* $\rho' \equiv \rho - \omega\left(\mathbb{E}\,e^{(1-\gamma)\cdot J_1} - 1\right)$*, and equation* (13) *continues to hold with* ρ *replaced by* $\rho'' \equiv \rho - \omega\left(\mathbb{E}\,e^{-\gamma\cdot J_1} - 1\right)$*.*

Proof. The global jumps condition implies that the CGF takes the form $\boldsymbol{c}(\boldsymbol{\theta}) = \boldsymbol{\theta}'\boldsymbol{\mu} + \boldsymbol{\theta}'\boldsymbol{\Sigma}\boldsymbol{\theta}/2 + \omega\left(\mathbb{E}\,e^{J_1(\theta_1+\theta_2)} - 1\right)$. In the case of the price-dividend ratio (4), we substitute $\theta_1 = 1 - \gamma/2 - iz$ and $\theta_2 = -\gamma/2 + iz$ into $\boldsymbol{c}(\boldsymbol{\theta})$; in the case of the riskless rate (9), we substitute $\theta_1 = -\gamma/2 - iz$ and $\theta_2 = -\gamma/2 + iz$. In each case, the sum $\theta_1 + \theta_2$ is independent of z, so the jump component of the CGF, $\omega\left(\mathbb{E}\,e^{J_1(\theta_1+\theta_2)} - 1\right)$, is a constant independent of z. We can therefore fold this constant into ρ, and the result follows. □

2.3 Two examples

I now present two numerical examples. The first is a conditionally lognormal model driven by Brownian motions, so the consumption-CAPM and ICAPM hold, and familiar intuition can be brought to bear. It is also easy to use Itô's lemma to calculate second-moment quantities such as betas and return volatilities, and I do so without further comment. The second example illustrates the effects of disastrous jumps, and is revisited later in the paper with $N > 2$. Dividend growth is independent and symmetrically distributed across assets in both examples, so that any correlations and asymmetries that emerge do so endogenously. I consider several different risk aversion parameters γ, and adjust the time preference rate ρ so that the long rate remains constant, at 7%, as γ varies. In each example, I consider the largest possible range of $\gamma \geq 1$ that is consistent with the finiteness assumptions in Table 1.

2.3.1 Dividends follow geometric Brownian motions

Suppose that the two assets have dividends which follow geometric Brownian motions. Each has mean log dividend growth of 2% and dividend volatility of 10%. In the notation of equation (2), $\mu_1 = \mu_2 = 0.02$, $\sigma_{11} = \sigma_{22} = 0.1^2$, and $\sigma_{12} = 0$. Because both assets have the same mean dividend growth, mean consumption growth does not vary with s. But the standard deviation of consumption growth does vary: it is lowest "in the middle", for $s = 0.5$, where there is most diversification. At the edges, where s is close to 0 or to 1, one of the two assets dominates the economy, and consumption growth is more volatile: the representative agent's eggs are all in one technological basket. Time-varying consumption growth volatility leads to a time-varying riskless rate. Figure 2a plots the riskless rate against asset 1's share of output s. Riskless rates are high for intermediate values of s because consumption volatility is low, which diminishes the motive for precautionary saving. Riskless rates also respond to changing expected consumption growth, with a sensitivity that depends on the elasticity of intertemporal substitution $1/\gamma$, but this channel is absent in the present example because mean consumption growth is constant.

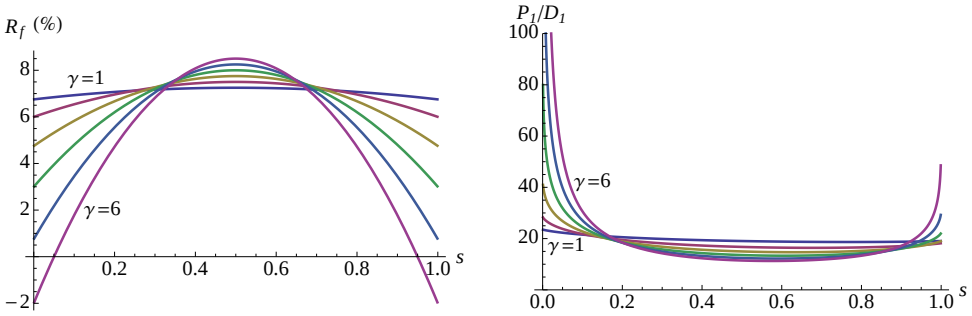

(a) Riskless rate (b) P/D

Figure 2: Left: Riskless rate. Right: Price-dividend ratio of asset 1.

Figure 2b shows the price-dividend ratio of asset 1 and of the market. When s is small, asset 1 contributes a small proportion of consumption. It therefore has little systematic risk, and hence a high valuation. As its dividend share increases, its discount rate increases both because the riskless rate increases and because its risk premium increases, as discussed further below. The model predicts that assets may have very high price-dividend ratios but not very low price-dividend ratios. Moreover, as an asset's share approaches zero, its price-dividend ratio becomes sensitively dependent on its share. I explore these issues further in Section 2.4.

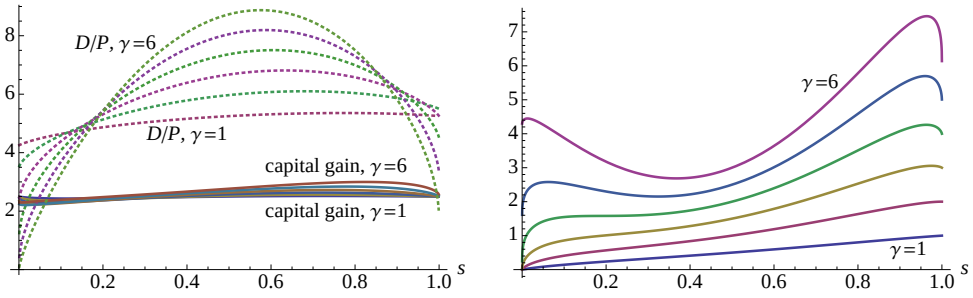

(a) Expected return decomposition

(b) Excess return on asset 1

Figure 3: Left: The two components of expected returns: expected capital gains (solid) and dividend yields (dashed). Right: Excess return on asset 1 against s.

Figure 3a decomposes expected returns into dividend yield plus expected capital gain. Most of the time-series and cross-sectional variation in expected returns can be attributed to changes in dividend yield rather than in expected capital gains.

Figure 3b shows how the risk premium on asset 1 varies with s for each γ. Holding s constant, the risk premium is monotonically increasing in γ. In the limit $s \to 1$, for example, we are back in a one-tree world in which the risk premium is the familiar $\gamma\sigma_{11}$, so at the right hand side of the figure the risk premia march up linearly as γ increases: 1%, 2%, ..., 6%. In contrast, for fixed s close to zero, asset 1's risk premium rises faster than linearly in γ. In this lognormal calibration the consumption-CAPM holds, so the risk premium depends on γ, on the correlation between asset 1 and consumption growth, $\kappa_{1,\Delta c}$, and on the volatility of asset 1's return σ_1 and of consumption growth $\sigma_{\Delta c}$: risk premium $= \gamma\kappa_{1,\Delta c}\sigma_1\sigma_{\Delta c}$. So two effects are in play. First, the *price* of risk, $\gamma\sigma_{\Delta c}$, increases linearly in γ. Second, asset 1's *quantity* of risk, $\kappa_{1,\Delta c}\sigma_1$, increases. This could be due either to an increase in the correlation of asset 1's return with consumption growth, or to an increase in the volatility of asset 1's return; it will turn out to be due to the former.

Now consider the behavior of the risk premium as s varies, holding γ constant. For γ between 1 and 4, the risk premium is monotonically increasing in s, and it tends to zero as s tends to zero, though for γ between 2 and 4 the risk premium rises very rapidly for s close to zero, so that even very small assets earn economically significant risk premia. For γ equal to 5 or 6, the risk premium is nonmonotonic, and tends to a strictly positive quantity as $s \to 0$. Again, this reflects the emergence of correlation despite the fact that, for small s, asset 1's fundamentals are almost uncorrelated with consumption growth. Thus

we have the interesting feature that as γ increases, asset prices behave *qualitatively*, not just quantitatively, differently. In the terminology of Section 2.4, where I explore this further, asset 1 is *subcritical* if $\gamma = 1$; subcritical but *nearly supercritical* if $\gamma = 2, 3, 4$; and *supercritical* if $\gamma = 5, 6$.

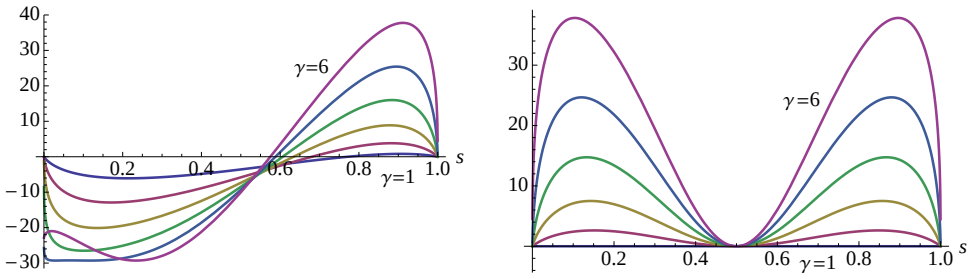

(a) Excess volatility of asset 1.

(b) Excess volatility of the market.

Figure 4: Left: Asset 1's excess return volatility relative to its (constant) dividend volatility. Right: The market's excess return volatility relative to its (nonconstant) dividend volatility.

At first sight it is surprising that asset 1's risk premium achieves its maximum at a value of s close to but strictly less than one. It does so because asset 1 has excess volatility at this point. Figure 4a plots the amount, in percentage points, by which asset 1's return volatility exceeds its dividend volatility. Asset 1's volatility is smaller than its dividend volatility for small s and larger for large s. Since the larger asset has a higher weight in the market, the model generates excess volatility in the aggregate market when $\gamma > 1$ (Figure 4b). With log utility, there is no excess volatility because the price-dividend ratio of the aggregate market is constant. For the same reason, there is no excess volatility when $s = 1/2$ or equivalently $u = 0$: the market price-dividend ratio is flat, as a function of u, at that point. Lastly, there is no excess volatility in the one-tree limits, $s = 0, 1$, or equivalently $u = -\infty$ or $+\infty$; again, the market price-dividend ratio is flat as a function of u in the limit.

In the two-asset case, two types of shock move an asset's price: a shock to its dividends, or a shock to the other asset's dividends, which changes the asset's price by changing its price-dividend ratio. Figure 5 plots the percentage price response of asset 1 (solid) and asset 2 (dashed) to a 1% increase in asset 1's dividends. When asset 1 is small, it underreacts to good news about its own cashflow shock and asset 2 moves in the opposite direction. When asset 1 is large, it overreacts to good news about its own cashflow shock, and asset 2 moves in the same direction. Note also that asset 2's price moves considerably more, in response to dividend news for asset 1, when asset 1 is large than when it is small. Again,

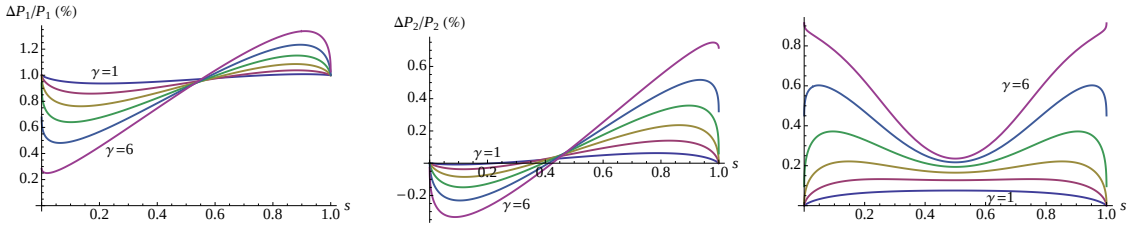

(a) Response of asset 1's price. (b) Response of asset 2's price. (c) Correlation between returns.

Figure 5: The response of assets 1 and 2 to a 1% increase in the dividend of asset 1; and the correlation in their returns.

the sizes of these effects are nonlinear in γ. For γ equal to 5 or 6, it is even possible for asset 1 to react more to asset 2's dividend than to its own (because for these values of γ, the response of asset 1's price at the left-hand side of Figure 5a is less than the response of asset 2's price at the right-hand side of Figure 5b; note that the setup is symmetrical). The result can be seen in Figure 5c: the two assets have highly correlated returns despite their independent fundamentals. The amount of correlation increases sharply with γ, especially when one asset is much larger than the other.

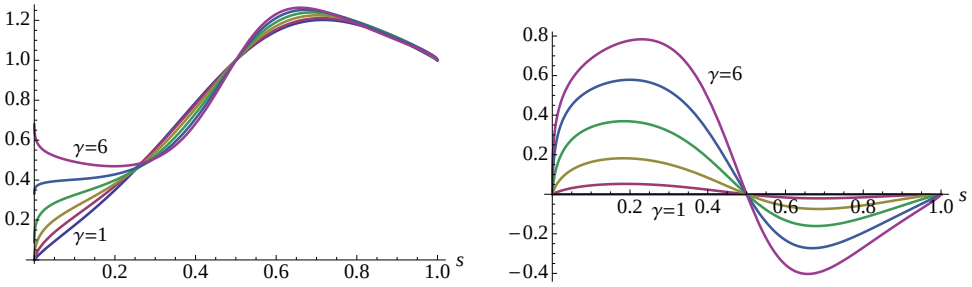

(a) Asset 1's CAPM beta (b) Asset 1's CAPM alpha

Figure 6: Asset 1's CAPM beta and alpha.

Since the consumption-CAPM holds in this calibration, an asset's risk premium lines up perfectly with the covariance of its return with consumption growth. On the other hand, the CAPM does not hold except in the log utility case $\gamma = 1$, so it is interesting to see the pattern of deviations from the CAPM that the model generates. Figure 6a plots asset 1's CAPM beta, $\operatorname{cov}_t(d\log P_1, d\log P_M) / \operatorname{var}_t d\log P_M$ (where P_M is the price of the market). It is mechanically equal to 1 when $s = 1$ (because asset 1 is the whole market) and when $s = 1/2$ (because assets 1 and 2 are identical, and hence have identical betas, which must

equal 1 because the aggregate market's beta equals 1). For the smaller values of γ, asset 1's beta declines towards zero fairly quickly as the asset's share goes to zero. But for the larger values of γ, asset 1 has a sizeable beta even in the limit as $s \to 0$ in which its fundamentals are independent of consumption growth. Figure 6b shows asset 1's CAPM alpha measured in percentage points, the difference between its true expected excess return and the excess return predicted by the CAPM. When $\gamma = 1$ the CAPM holds so alpha is zero for all s. For larger values of γ, asset 1's alpha is mechanically zero at the two end points (because in a one-tree world, the market return is perfectly correlated with consumption growth, so the CAPM holds) and at $s = 1/2$ (because the two assets are identical, so their alphas must both be zero). As asset 1's share increases from zero, its price-dividend ratio drops sharply and its alpha increases sharply. Since the aggregate market's alpha is zero, this means that alpha drops below zero as s decreases below 1.

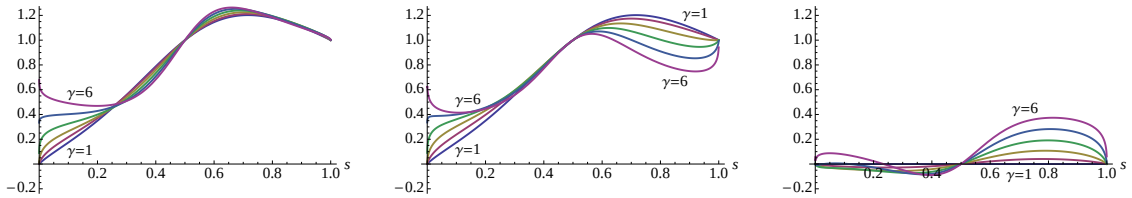

(a) CAPM beta, β (b) Cashflow beta, β_{CFM} (c) Discount-rate beta, β_{DRM}

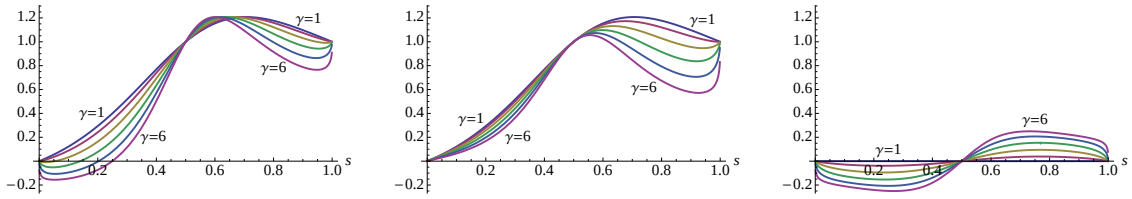

(d) β_{CF1} (e) $\beta_{CF1,CFM}$ (f) $\beta_{CF1,DRM}$

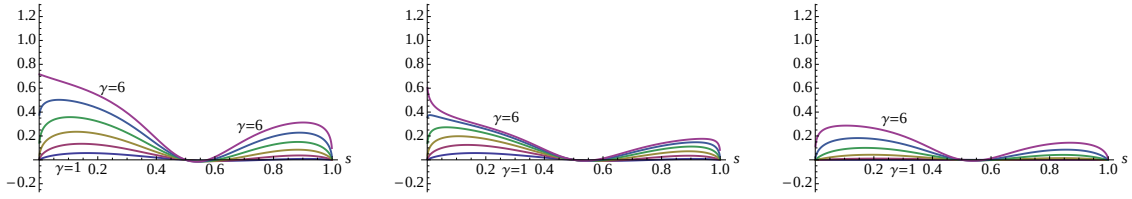

(g) β_{DR1} (h) $\beta_{DR1,CFM}$ (i) $\beta_{DR1,DRM}$

Figure 7: Beta decomposition.

What is the source of the small asset's high beta? To answer this question, it is useful to split asset 1's return into one part due to shocks to its cashflow, and another part due

to shocks to its valuation ratio, and to explore how each covaries with the market return:

$$\underbrace{\frac{\text{cov}_t\left(d\log P_1, d\log P_M\right)}{\text{var}_t\, d\log P_M}}_{\text{CAPM beta, }\beta} = \underbrace{\frac{\text{cov}_t\left(d\log D_1, d\log P_M\right)}{\text{var}_t\, d\log P_M}}_{\beta_{CF1}} + \underbrace{\frac{\text{cov}_t\left(d\log \frac{P_1}{D_1}, d\log P_M\right)}{\text{var}_t\, d\log P_M}}_{\beta_{DR1}}. \tag{14}$$

This is analogous to the exercise carried out by Campbell and Mei (1993) who asked, where do betas come from? Figures 7d and 7g report β_{CF1} and β_{DR1} in the model. The two figures add up to CAPM beta, shown in Figure 7a. As asset 1 gets larger, an increasingly large proportion of its CAPM beta is due to covariation between its fundamentals and the market return. In contrast, a very small asset's beta is almost entirely due to covariation between its valuation and the market return. The importance of valuation effects is particularly pronounced if γ is large.

To understand where *alphas* come from, we can slice CAPM beta up in a different way, splitting the *market's* return into a cashflow component and a valuation component:

$$\underbrace{\frac{\text{cov}_t\left(d\log P_1, d\log P_M\right)}{\text{var}_t\, d\log P_M}}_{\text{CAPM beta}} = \underbrace{\frac{\text{cov}_t\left(d\log P_1, d\log C\right)}{\text{var}_t\, d\log P_M}}_{\text{cashflow beta, }\beta_{CFM}} + \underbrace{\frac{\text{cov}_t\left(d\log P_1, d\log \frac{P_M}{C}\right)}{\text{var}_t\, d\log P_M}}_{\text{discount-rate beta, }\beta_{DRM}}. \tag{15}$$

This expression breaks the conventional CAPM beta into a cashflow beta that measures the covariance of the asset's return with shocks to the aggregate market's cashflows, and a discount-rate beta that measures the covariance of the asset's return with shocks to the aggregate market's valuation ratio. It is the continuous-time version of the good-beta/bad-beta decomposition of Campbell and Vuolteenaho (2004). In a loglinear approximation of a homoskedastic conditionally lognormal model, Campbell (1993) derives an ICAPM result whose continuous-time analogue is that

$$RP = \gamma\sigma^2\beta_{CFM} + \sigma^2\beta_{DRM}, \tag{16}$$

where RP_1 denotes asset 1's instantaneous risk premium, σ^2 is the instantaneous variance of the market return, and β_{CFM} and β_{DRM} were defined in (15). The online Appendix shows that (16) holds to high accuracy in the present calibration. Figures 7b and 7c plot cashflow beta and discount-rate beta against s. For small assets, CAPM beta is composed almost entirely of ("bad") cashflow beta. When $\gamma = 1$, discount-rate beta is zero across the whole range of s—hence CAPM beta is identically equal to cashflow beta—because with log utility the consumption-wealth ratio, i.e. the market's valuation ratio, is constant. For larger values of γ, ("good") discount-rate beta becomes a significant contributor once asset

1 is large. Since discount-rate beta earns a lower risk premium than cashflow beta, large assets earn negative alphas and small assets earn positive alphas.

To understand why the cashflow and discount-rate betas look as they do, we can do a further decomposition that, essentially, combines (14) and (15), splitting the returns on both asset 1 *and* the market into cashflow and discount-rate components. (Campbell, Polk and Vuolteenaho (2010) carry out this completing-the-square exercise.) Doing so, we see that cashflow betas are high for a small asset because the small asset's *discount rate* covaries strongly with the market's cashflows (Figures 7e and 7h). The picture is more mixed regarding a small asset's discount-rate beta. There are two forces pulling in opposite directions: a small asset's *cashflows* covary negatively with market discount rates (Figure 7f), while its *discount rate* covaries positively with market discount rates (Figure 7i).

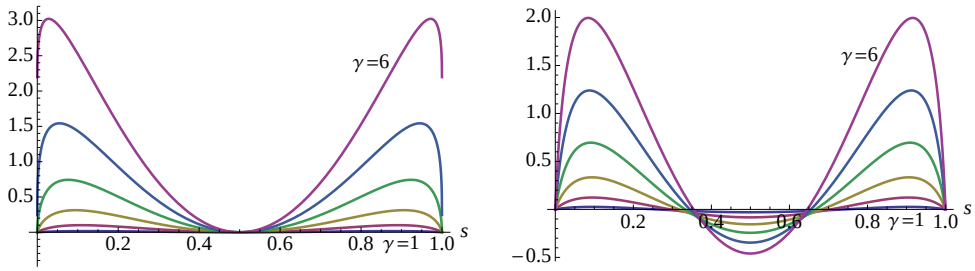

(a) Excess returns on a perpetuity.

(b) The yield spread.

Figure 8: A high yield spread signals high expected excess returns on a perpetuity.

Finally, we can consider the behavior of bonds in zero net supply. Figure 8a plots the risk premium on a real perpetuity which pays one unit of consumption good per unit time. Bonds are risky because bad times—i.e., bad news for the larger asset, whether asset 1 or 2—are associated with the state variable moving towards $s = 1/2$, and hence with a rise in the riskless rate and a fall in bond prices. Figure 8b shows how the spread in yields between a 30-year zero-coupon bond and the instantaneous riskless rate varies with s. A high yield spread forecasts high excess returns on long-term bonds.

2.3.2 Dividends are subject to occasional disasters

The second example briefly highlights the effect of disasters; it will be explored further in a three-asset example below. In addition to the two Brownian motions driving dividends, there are also jumps in dividends, representing the occurrence of disasters. Jumps arrive, independently across assets, at rate 0.017—on average, about once every 60 years. When

a disaster strikes an asset, it shocks its log dividend by a Normal random variable with mean -0.38 and standard deviation 0.25. These disaster arrival rates—and the mean and standard deviation of the disaster sizes—are chosen to match exactly the empirical disaster frequency estimated by Barro (2006), and to match approximately the disaster size distribution documented in the same paper. I adjust the drifts μ_1 and μ_2, and the Brownian variances σ_{11} and σ_{22}, so that the mean and variance of each asset's log dividend growth are the same as in the previous example.

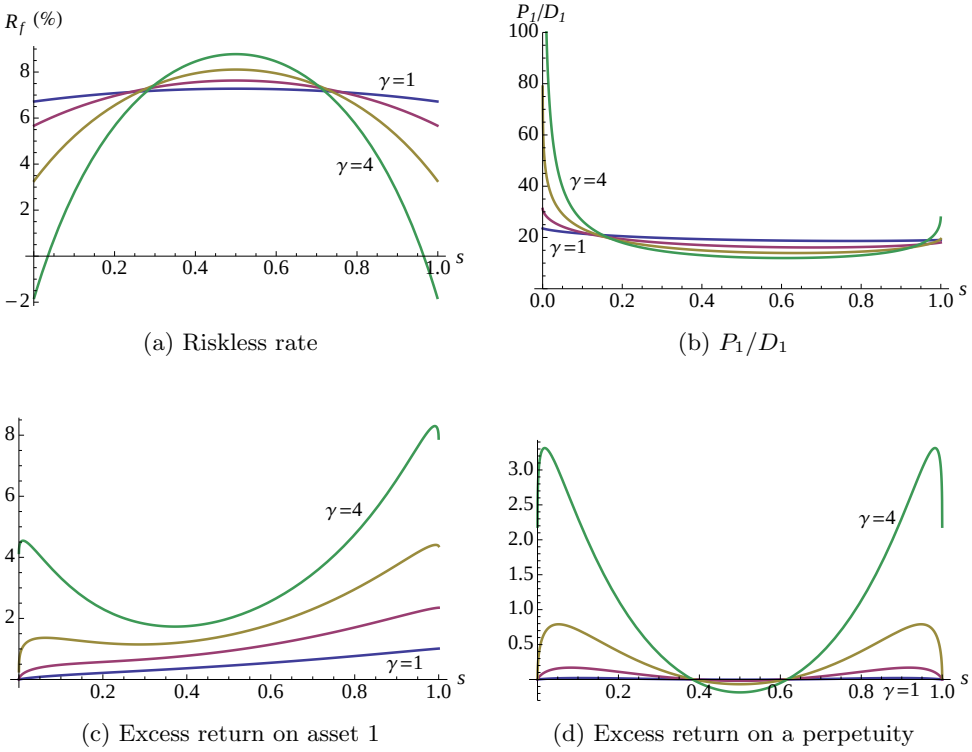

(a) Riskless rate

(b) P_1/D_1

(c) Excess return on asset 1

(d) Excess return on a perpetuity

Figure 9: The disaster calibration.

Figure 9 shows that, holding γ constant, the riskless rate is lower and the risk premium higher than in the jump-free example for most values of s. As in Rietz (1988) and Barro (2006), incorporating rare disasters makes it easier to match observed riskless rates and risk premia without requiring implausibly large γ. Note, though, that with power utility, disasters lead to far more variation in the riskless rate.

Another feature distinctive to jumps is that disasters propagate to apparently safe assets: when the state variable jumps, interest rates and bond prices jump too. As a result the risk premium on a perpetuity is considerably higher than before when the current riskless

rate is low (for s close to 0 or 1), even though disasters do not affect its cashflows; and relative to the previous calibration, disasters have a much larger effect on the perpetuity's risk premium than on asset 1's risk premium.

As in the previous example, the riskless rate is locally constant at $s = 1/2$. Nonetheless, the perpetuity earns a negative risk premium there because it is a hedge against disasters: when a disaster strikes one of the assets, the riskless rate jumps down and the perpetuity's price jumps up. In the previous example, by contrast, the perpetuity was riskless at $s = 1/2$ because without jumps, the state variable could only move locally.

2.4 Equilibrium pricing of a small asset

A distinctive qualitative prediction of the model is that there should exist extreme growth assets, but not extreme value assets, as shown in Figure 2b. The extreme growth case also represents the starkest departure from simple models in which price-dividend ratios are constant (as in a one-tree model with power utility and i.i.d. dividend growth). Finally, it is important to understand whether the complicated dynamics exhibited above are relevant for assets that are small relative to the aggregate economy. This section therefore explores the price behavior of asset 1 in the limit $s \to 0$.[4]

Consider the problem of pricing a negligibly small asset whose fundamentals are independent of consumption growth in an environment in which the (real) riskless rate is 6%. If the small asset has mean dividend growth rate of 4%, the following logic seems plausible. Since the asset is negligibly small and idiosyncratic, it need not earn a risk premium, so the appropriate discount rate is the riskless rate. Next, since dividends are i.i.d., it seems sensible to apply the Gordon growth model to conclude that dividend yield = riskless rate − mean dividend growth = 2%. This argument can be made formal, and I do so below. Now consider the empirically more relevant situation in which the riskless real rate is 2%. If the asset does not earn a risk premium, the Gordon growth model seems to suggest that the dividend yield should be $2\% - 4\% = -2\%$, a nonsensical result.

To investigate this issue, I return to the general setup and make a definition.

Definition 3. *If the inequality*

$$\rho - \boldsymbol{c}(1, -\gamma) > 0 \tag{17}$$

[4]In this section I assume that $\widetilde{\boldsymbol{y}}_1$ has uncountable essential support, so that Lemma 3 applies. This is an extremely weak assumption. The only remotely natural case in which it fails is if log dividends follow a pure jump process with jumps of fixed size.

holds, we are in the subcritical *case, while if the inequality*

$$\rho - \boldsymbol{c}(1, -\gamma) < 0 \tag{18}$$

holds, we are in the supercritical *case.*[5]

The supercritical regime occurs if ρ is sufficiently small, γ sufficiently large, or if fundamentals are sufficiently risky, in the sense that the CGF has large curvature.[6] Consider, for example, the case in which dividend growth is independent across assets, so that the risk in question is both small and idiosyncratic. Conditions (17) and (18) can then be given a simple interpretation, since the CGF decomposes as $\boldsymbol{c}(\theta_1, \theta_2) = \boldsymbol{c}_1(\theta_1) + \boldsymbol{c}_2(\theta_2)$ where $\boldsymbol{c}_i(\theta_i) \equiv \log \mathbb{E} \exp\{\theta_i(\widetilde{y}_{i,t+1} - \widetilde{y}_{i,t})\}$, so

$$\rho - \boldsymbol{c}(1, -\gamma) = \rho - [\boldsymbol{c}_1(1) + \boldsymbol{c}_2(-\gamma)] = \underbrace{\rho - \boldsymbol{c}(0, -\gamma)}_{\overline{R_f}} - \underbrace{\boldsymbol{c}(1, 0)}_{G_1}.$$

More generally, if the assets are not independent, conditions (17) and (18) allow for the fact that asset 1 earns a risk premium. In the lognormal case, for example,

$$\rho - \boldsymbol{c}(1, -\gamma) = \overline{R_f} + \underbrace{\gamma \operatorname{cov}(\Delta y_{1,t+1}, \Delta c_{t+1})}_{\text{risk premium}} - G_1.$$

Thus the subcritical case applies whenever the Gordon growth model produces a reasonable—meaning positive—dividend yield, and the supercritical case applies when the Gordon growth model breaks down, predicting a negative dividend yield.

The next result gives various asymptotics in the two cases. Bars above variables indicate limits as $s \to 0$, so for example $\overline{R_f} = \lim_{s \to 0} R_f(s)$. To highlight the link with the traditional Gordon growth formula, I write $G_1 \equiv \boldsymbol{c}(1, 0)$ and $G_2 \equiv \boldsymbol{c}(0, 1)$ for (log) mean dividend growth on assets 1 and 2 respectively, and $\overline{R_1}$ and $\overline{R_2}$ for the limiting expected instantaneous returns on assets 1 and 2. Finally, I write $\overline{XS_1}$ for the limiting excess return on asset 1.

Proposition 6. *As $s \to 0$ the Gordon growth model, $\overline{D/P_2} = \overline{R_2} - G_2$, holds for the large*

[5] There is also a knife-edge *critical* case in which $\rho - \boldsymbol{c}(1, -\gamma) = 0$ and $z^* = \gamma/2$. The simple example in Section 1 of Cochrane, Longstaff and Santa-Clara (2008) is critical. This is no coincidence: the condition that implies criticality also ensures that the expression for the price-dividend ratio is relatively simple.

[6] In the lognormal case with $\gamma = 1$, condition (18) reduces to a simplified version of Cochrane, Longstaff and Santa-Clara's (2008) condition $\theta \leq 1$. With log utility and lognormal dividend growth, though, the supercritical case only occurs in rather unusual calibrations.

asset in either the subcritical or supercritical case, and we have

$$\begin{aligned}\overline{R_f} &= \rho - \boldsymbol{c}(0, -\gamma) \\ \overline{D/P_2} &= \rho - \boldsymbol{c}(0, 1-\gamma) \\ \overline{XS_2} &= \boldsymbol{c}(0,1) + \boldsymbol{c}(0,-\gamma) - \boldsymbol{c}(0, 1-\gamma).\end{aligned}$$

In the subcritical *case, the Gordon growth model also holds for the small asset:* $\overline{D/P_1} = \overline{R_1} - G_1$. *We have*

$$\begin{aligned}\overline{D/P_1} &= \rho - \boldsymbol{c}(1, -\gamma) \\ \overline{XS_1} &= \boldsymbol{c}(1,0) + \boldsymbol{c}(0,-\gamma) - \boldsymbol{c}(1, -\gamma).\end{aligned}$$

If the two assets have independent fundamentals, then $0 = \overline{XS_1} < \overline{XS_2}$.

In the supercritical *case, the Gordon growth model fails, and we have*

$$\begin{aligned}\overline{D/P_1} &= 0 \\ \overline{XS_1} &= \boldsymbol{c}(1-\gamma/2+z^*, \gamma/2-z^*) + \boldsymbol{c}(0,-\gamma) - \boldsymbol{c}(1-\gamma/2+z^*, -\gamma/2-z^*) \quad (19)\end{aligned}$$

where z^* *is the unique positive root of* $\phi(z) \equiv \rho - \boldsymbol{c}(1-\gamma/2+z, -\gamma/2-z)$, *so*

$$\rho - \boldsymbol{c}(1-\gamma/2+z^*, -\gamma/2-z^*) = 0. \quad (20)$$

If $G_1 \geq G_2$, *then* $\overline{D/P_1} \geq \overline{R_1} - G_1$. *If the assets have independent fundamentals, then* $0 < \overline{XS_1} < \overline{XS_2}$.

Sketch proof. (Here I outline the proof for the small asset, which is the more interesting of the two. See Appendix A.5 for the full proof.) The basic idea is that the behavior of the integrals (4), (7) and (9) in the small-asset limit $u \to \infty$ is determined only by the residue at the *minimal pole* whose imaginary part is closest to zero, because poles with larger imaginary parts are asymptotically irrelevant due to the e^{iuz} term. I show this by integrating around a contour which avoids all poles except for this minimal pole.

The key issue is the precise location of the minimal pole. In the case of the riskless rate, the minimal pole of the integrand in (9) is at the minimal pole of $\mathscr{F}_\gamma(z)$, which lies at $(\gamma/2)i$ by standard properties of the Γ-function. In the case of the price-dividend ratio (4) or expected return (7), the minimal pole of the integrand could occur at $(\gamma/2)i$, but there is also the possibility that it occurs at the minimal zero of $\rho - \boldsymbol{c}(1-\gamma/2-iz, -\gamma/2+iz)$. Lemma 3 in Appendix A.3 shows that such a minimal zero must lie on the imaginary axis, at z^*i,

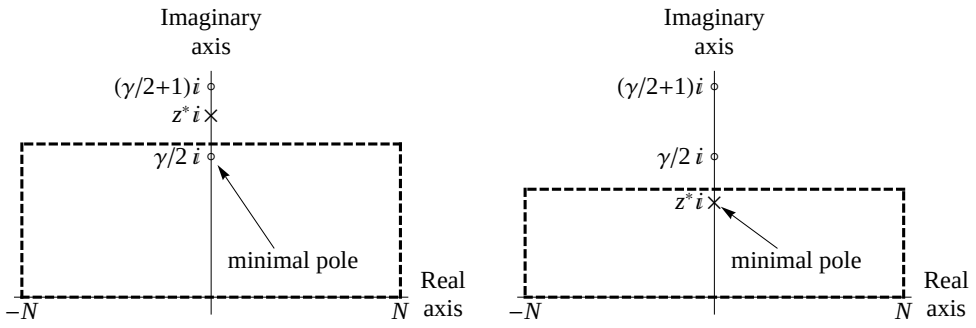

(a) Subcritical case (b) Supercritical case

Figure 10: The contour of integration in the subcritical and supercritical cases.

say. If there is such a zero, then z^* is a solution to (20), and is unique by convexity of $\boldsymbol{c}(\cdot,\cdot)$. The question is whether z^*, if it exists, is larger or smaller than $\gamma/2$. In the subcritical case, z^* may or may not exist, but it certainly cannot be smaller than $\gamma/2$ because ϕ is concave, and positive at $z=0$ and at $z=\gamma/2$ by the finiteness and subcriticality conditions respectively. So the minimal pole of the integrand occurs at $(\gamma/2)i$, and the desired result follows on computing the residue there; this is the less interesting case. In the supercritical case, $\phi(z)$ is now *negative* at $z=\gamma/2$ by the supercriticality condition (18). Therefore there is a unique z^* solving (20), by the intermediate value theorem and concavity of ϕ, and the location of the minimal pole is at z^*i.

The two alternatives are illustrated in Figure 10, which indicates poles of $\mathscr{F}_\gamma(z)$ with circles and marks the pole due to the zero of $\rho-\boldsymbol{c}(1-\gamma/2-iz,-\gamma/2+iz)$ with a cross. (Not all poles are shown: for example, $\mathscr{F}_\gamma(z)$ has poles at $(\gamma/2+m)i$ for all nonnegative integer m. There may also be other poles due to zeros of $\rho-\boldsymbol{c}(1-\gamma/2-iz,-\gamma/2+iz)$; if so, they must lie off the imaginary axis and have imaginary parts greater than z^*.) For the sake of argument, consider the effect of increasing patience on the part of the representative agent, i.e. decreasing ρ. Starting from a high value of ρ, z^* is large (left panel). As ρ declines, the cross indicating the pole at z^*i moves smoothly down the axis. After it crosses $(\gamma/2)i$, it becomes the minimal pole (right panel), and there is a qualitative change in the behavior of asset 1, which becomes supercritical.

Figures 10a and 10b also show the rectangular contours around which we integrate. As $N\to\infty$, the integral along the base of the rectangle tends to the integral we want, and the contribution of the other three sides becomes negligible. □

The large asset's valuation ratio and excess return, and the riskless rate, are determined

only by the characteristics of the large asset's dividend process, and by formulas that are exactly analogous to those derived in Martin (2008).

The small asset is more interesting because there is no economic reason to impose the constraint that its price-dividend ratio should be finite in the limit.[7] If it *is*, in the subcritical case, then the small asset obeys the Gordon growth formula, and earns no risk premium if its dividends are independent of the large asset's dividends (and hence of consumption).

In the supercritical regime, on the other hand, the small asset has an enormous valuation ratio—reminiscent of Pástor and Veronesi (2003, 2006)—and one that is sensitively dependent on its dividend share. As a result, when the large asset has bad news, the small asset falls down the valuation curve, hence comoves. This means that the small asset earns a strictly positive risk premium even if its fundamentals are independent of the large asset's fundamentals (and hence of consumption). Moreover, the expected return on the asset is entirely due to expected capital gains, because the asset's dividend yield is zero in the limit.

The next result refines the previous one by showing what happens near, not just *at*, the limit. When $z^* > \gamma/2 + 1$, the riskless rate, price-dividend ratio and excess return of the small asset are approximately affine functions of s. Things are more interesting in the supercritical case and in the *nearly supercritical* case in which $\gamma/2 < z^* < \gamma/2 + 1$, so I now restrict to these cases. The notation $a \doteq b$ means "a equals b plus higher order terms in s".

Proposition 7. *The riskless rate is given, to leading order in s, by*

$$R_f \doteq A_1 + B_1 \cdot s.$$

In the nearly supercritical case, the dividend yield and excess return satisfy

$$\begin{aligned} D/P_1 &\doteq A_2 + B_2 \cdot s^{|z^* - \gamma/2|} \\ XS_1 &\doteq A_3 + B_3 \cdot s^{|z^* - \gamma/2|}. \end{aligned}$$

In the supercritical case, the dividend yield and excess return are given by

$$\begin{aligned} D/P_1 &\doteq B_4 \cdot s^{|z^* - \gamma/2|} \\ XS_1 &\doteq A_5 + B_5 \cdot s^{|z^* - \gamma/2|} \end{aligned}$$

[7] In contrast, there *is* an economic reason to impose a finite price-*consumption* ratio in the limit. Since $P_1/C = D_1/(D_1 + D_2) \cdot P_1/D_1 = s \cdot P_1/D_1$, the price-consumption ratio will tend to zero if P_1/D_1 tends to infinity more slowly than s tends to zero. Appendix A.5 shows that this holds so long as $\rho - \boldsymbol{c}(0, 1-\gamma) > 0$, i.e., so long as the price-dividend ratio of the *large* asset is finite in the limit. This is one of the finiteness assumptions in Table 1.

where the constants A_i were given in Proposition 6, and the constants B_i are given in Appendix A.5.1. Dividend yields are increasing in share, $B_2 > 0$ and $B_4 > 0$.

If the assets have independent fundamentals, then excess returns increase in share, too: $A_3 = 0$ and $B_3 > 0$ in the nearly supercritical case, and $A_5 > 0$ and $B_5 > 0$ in the supercritical case.

This result has three immediate implications. First, the exponent $|z^* - \gamma/2|$ is between zero and one, so $s^{|z^*-\gamma/2|}$ is *much larger* than s when $s \approx 0$: its derivative with respect to s is infinite at zero. Thus near the small-asset limit, the small asset's price-dividend ratio and risk premium are *far* more sensitive to changes in s than the riskless rate is. In particular, changes in price-dividend ratio—which, mechanically, are associated with changes in expected returns, since dividend growth is unforecastable—can be attributed more specifically to changes in expected excess returns as opposed to changes in interest rates. Cochrane (2005, p. 400) emphasizes that this is a feature of the data. Second, the small asset's price-dividend ratio is decreasing in its share, and so comoves positively in response to shocks to the large asset's dividend, no matter what we assume about the dividend processes of the two assets or the correlation between the two. Finally, in the supercritical case, the small asset's log *price-dividend ratio* follows a random walk—more precisely, a Lévy process. For, since $s_t \sim e^{-u_t}$ in the small-asset limit, we have

$$\log P/D_{1t} \doteq -\underbrace{\log B_4}_{\text{constant}} + |z^* - \gamma/2|\, u_t. \tag{21}$$

If log dividends follow Brownian motions, for example, then so does $\log P/D_{1,t}$. This is why (19)—which can be rephrased as $\overline{ER}_1 = \boldsymbol{c}(1 - \gamma/2 + z^*, \gamma/2 - z^*)$—takes the form it does: by (21), it is expressing the fact that $\overline{ER}_1 = \log \mathbb{E}\left[\frac{D_{1,t+1}}{D_{1,t}} \frac{P_{1,t+1}/D_{1,t+1}}{P_{1,t}/D_{1,t}}\right] = \log \mathbb{E}\left[\frac{P_{1,t+1}}{P_{1,t}}\right]$.

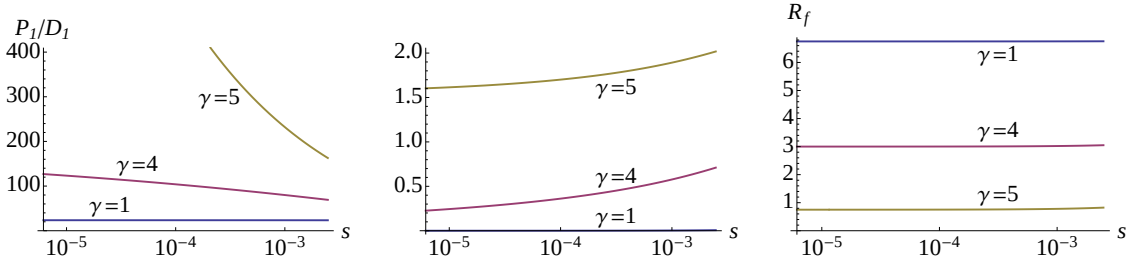

(a) Asset 1's P/D ratio (b) Asset 1's excess return (c) Riskless rate

Figure 11: The price-dividend ratio of a small asset, its excess return, and the riskless rate.

Figure 11 shows zoomed-in versions of some of the figures from Section 2.3.1, to exhibit

these phenomena in the Brownian-motion-driven example considered there. This should make it clear both that the supercritical case does not require extreme parameter values and that the magnitudes of the effects are economically meaningful. To recap, the world is symmetric, and the two assets are independent with 2% mean dividend growth and 10% dividend volatility. The small asset is not nearly supercritical if $\gamma = 1$; is nearly supercritical if $\gamma = 2, 3$ or 4; and is supercritical if $\gamma = 5$ or 6. To keep the graphs readable, I plot $\gamma = 1, 4$ and 5 as representatives of the three possibilities. As always, I adjust ρ so that the long rate is 7%. In each case, the riskless rate is essentially constant over the range plotted. When $\gamma = 1$, asset 1's price-dividend ratio and excess return are effectively constant. When $\gamma = 4$, the price-dividend ratio almost doubles (from 69 to 127) over the range plotted and the excess return varies between about 25bp and 75bp. When $\gamma = 5$, the price-dividend ratio explodes and the time-varying excess return remains above 1.5% even in the limit.

3 N assets

The basic approach is the same with $N > 2$ assets. The main technical difficulty lies in calculating $\mathscr{F}_\gamma^N(\boldsymbol{z}) \equiv \mathscr{F}_\gamma^N(z_1, \ldots, z_{N-1})$, the generalization of $\mathscr{F}_\gamma(z)$ to the N-tree case. It turns out that we have

$$\mathscr{F}_\gamma^N(\boldsymbol{z}) = \frac{\Gamma\left(\gamma/N + iz_1 + iz_2 + \ldots + iz_{N-1}\right)}{(2\pi)^{N-1}\Gamma(\gamma)} \cdot \prod_{k=1}^{N-1} \Gamma\left(\gamma/N - iz_k\right).$$

Before stating the main result, it will be useful to recall some old, and to define some new, notation. Let $\boldsymbol{e}_j$ be an N-vector with a one at the jth entry and zeros elsewhere, and define the N-vectors $\boldsymbol{y}_0 \equiv (y_{10}, \ldots, y_{N0})'$ and $\boldsymbol{\gamma} \equiv (\gamma, \ldots, \gamma)'$, and the $(N-1) \times N$ matrix $\boldsymbol{U}$ and the $(N-1)$-vector $\boldsymbol{u}$ by

$$\boldsymbol{U} \equiv \begin{pmatrix} -1 & 1 & 0 & \cdots & 0 \\ -1 & 0 & 1 & \ddots & \vdots \\ \vdots & \vdots & \ddots & \ddots & 0 \\ -1 & 0 & \cdots & 0 & 1 \end{pmatrix} \quad \text{and} \quad \boldsymbol{u} \equiv \begin{pmatrix} u_2 \\ u_3 \\ \vdots \\ u_N \end{pmatrix} \equiv \boldsymbol{U}\boldsymbol{y}_0 = \begin{pmatrix} y_{20} - y_{10} \\ y_{30} - y_{10} \\ \vdots \\ y_{N0} - y_{10} \end{pmatrix}. \tag{22}$$

In the two-asset case, the state variable was one-dimensional. With N assets, a natural set of state variables is $\{s_i\}_{i=1,\ldots,N-1}$, where $s_i = D_{i0}/(D_{10} + \cdots + D_{N0})$ is the dividend share of asset i; it turns out, though, to be more convenient to work with the $(N-1)$-dimensional state vector $\boldsymbol{u}$. The first entry of $\boldsymbol{u}$ is $u_2 = y_{20} - y_{10}$, which corresponds to the

state variable u of previous sections. More generally, $u_k = y_{k0} - y_{10}$ is a measure of the size of asset k relative to asset 1. Consistent with this notation, I write $u_1 \equiv y_{10} - y_{10} = 0$ and define the N-vector $\boldsymbol{u}_+ \equiv (u_1, u_2, \ldots, u_N)' = (0, u_2, \ldots, u_N)'$ to make some formulas easier to read.

The following Proposition generalizes earlier integral formulas to the N-asset case. All integrals are over $\mathbb{R}^{N-1}$. The condition that ensures finiteness of the price of asset j is that $\rho - \boldsymbol{c}(\boldsymbol{e}_j - \boldsymbol{\gamma}/N) > 0$. I assume that this inequality holds for all j.

Proposition 8. *The price-dividend ratio on asset j is*

$$P/D = e^{-\boldsymbol{\gamma}'\boldsymbol{u}_+/N} \left(e^{u_1} + \cdots + e^{u_N}\right)^\gamma \int \frac{\mathscr{F}_\gamma^N(\boldsymbol{z}) e^{i\boldsymbol{u}'\boldsymbol{z}}}{\rho - \boldsymbol{c}(\boldsymbol{e}_j - \boldsymbol{\gamma}/N + i\boldsymbol{U}'\boldsymbol{z})}\, d\boldsymbol{z}.$$

Defining the expected return by $ER\,dt \equiv \mathbb{E}(dP + D\,dt)/P$, we have

$$ER = \frac{\Phi}{P/D} + D/P,$$

where

$$\Phi = \sum_{\boldsymbol{m}} \binom{\gamma}{\boldsymbol{m}} e^{(\boldsymbol{m} - \boldsymbol{\gamma}/N)'\boldsymbol{u}_+} \int \frac{\mathscr{F}_\gamma^N(\boldsymbol{z}) e^{i\boldsymbol{u}'\boldsymbol{z}} \boldsymbol{c}(\boldsymbol{e}_j + \boldsymbol{m} - \boldsymbol{\gamma}/N + i\boldsymbol{U}'\boldsymbol{z})}{\rho - \boldsymbol{c}(\boldsymbol{e}_j - \boldsymbol{\gamma}/N + i\boldsymbol{U}'\boldsymbol{z})}\, d\boldsymbol{z}.$$

The sum is over all vectors $\boldsymbol{m} = (m_1, \ldots, m_N)'$ whose entries are non-negative integers that add up to γ. I write $\binom{\gamma}{\boldsymbol{m}}$ for the multinomial coefficient $\gamma!/(m_1! \cdots m_N!)$.

The zero-coupon yield to time T is

$$\mathscr{Y}(T) = \rho - \frac{1}{T} \log \left[e^{-\boldsymbol{\gamma}'\boldsymbol{u}_+/N} \left(e^{u_1} + \cdots + e^{u_N}\right)^\gamma \int \mathscr{F}_\gamma^N(\boldsymbol{z}) e^{i\boldsymbol{u}'\boldsymbol{z}} e^{\boldsymbol{c}(-\boldsymbol{\gamma}/N + i\boldsymbol{U}'\boldsymbol{z})T}\, d\boldsymbol{z} \right].$$

The riskless rate is

$$r = e^{-\boldsymbol{\gamma}'\boldsymbol{u}_+/N} \left(e^{u_1} + \cdots + e^{u_N}\right)^\gamma \int \mathscr{F}_\gamma^N(\boldsymbol{z}) e^{i\boldsymbol{u}'\boldsymbol{z}} \left[\rho - \boldsymbol{c}(-\boldsymbol{\gamma}/N + i\boldsymbol{U}'\boldsymbol{z})\right]\, d\boldsymbol{z}.$$

These formulas can be expressed in terms of the dividend shares $\{s_i\}$ by making the substitution $u_k = \log(s_k/s_1)$.

Unfortunately, I have not been able to make any further analytical progress from these results, so I now resort to numerical evaluation of these integral formulas in an example with $N = 3$ trees. This is the largest N that can easily be represented graphically. I use the calibration of Section 2.3.2 with independent and symmetric fundamentals, $\gamma = 4$, and ρ set so that the long rate is 7%, as before.

Figure 12 shows three contour plots on the unit simplex. At the each corner of the simplex, one asset is dominant, $N = 1$. The top corner represents the state $(s_1, s_2, s_3) = (1, 0, 0)$; the bottom left corner represents $(s_1, s_2, s_3) = (0, 1, 0)$; and the bottom right corner represents $(s_1, s_2, s_3) = (0, 0, 1)$. Along the edges, two assets are dominant, $N = 2$. Light regions represent larger values and dark regions represent smaller values.

Figure 12a shows the riskless rate. The contours indicate riskless rates of $8\%, 6\%, \ldots, -2\%$, radiating outwards from the center. The figure is symmetric because the calibration is symmetric. As in the two-asset case, the riskless rate is highest in the middle, where the three assets have the same size, and lowest in the corners, where the economy is dominated by just one asset. Along the edges, we have copies of Figure 9a.

Figure 12b plots asset 1's excess return over the simplex. The contours indicate excess returns of $1\%, 2\%, \ldots, 8\%$. Since the calibration is symmetric, we can also read off the excess returns of assets 2 and 3 from the figure, by relabelling appropriately. If asset 1 is dominant, it has a high risk premium, and as its share declines, its risk premium declines; this is familiar. But as asset 1 becomes small, two distinct regimes emerge. If the economy is reasonably well balanced, in the sense that assets 2 and 3 are of roughly similar size, then the riskless rate is fairly high. In this situation, asset 1's risk premium tends to zero as its share approaches zero. But towards either of the bottom corners, where the economy is unbalanced, the riskless rate is low—lower than asset 1's mean dividend growth rate—and asset 1's valuation is high and sensitively dependent on dividend news for whichever asset dominates the economy. As a result of this endogenous positive comovement, it requires a sizeable risk premium even though its dividend is uncorrelated with consumption growth. This effect is enhanced because of disasters: when the large asset suffers a disaster, the small asset also suffers a "valuation disaster". I will refer to the two regimes as subcritical and supercritical, respectively, by analogy with Section 2.4. A new feature that arises once $N > 2$ is that an asset can be either subcritical or supercritical depending on where we are in the state space.

Figure 12c plots asset 1's price-dividend ratio. The contours are at price-dividend ratios of $14, 17, 20, \ldots, 35$. The price-dividend ratio is lowest between the top corner and the middle of the diagram, where the riskless rate is high because the world is well balanced and the risk premium on asset 1 is high because it is relatively large. As asset 1 becomes dominant, towards the top corner, the price-dividend ratio increases slightly from its minimum as the riskless rate drops more rapidly than asset 1's risk premium rises. When asset 1 is very small, there are two possibilities, as noted in the previous paragraph. In the subcritical

regime in which assets 2 and 3 are well-balanced, asset 1's price-dividend ratio increases towards a finite limit as its share and risk premium tend to zero. But in the supercritical regime in which one of assets 2 or 3 dominates the market, so that the riskless rate is low, asset 1's price-dividend ratio can grow unboundedly as its share approaches zero, which is why no contours are plotted near the bottom corners. Along the bottom edge of the simplex, therefore, asset 1's dividend yield and excess return move in opposite directions as it shifts from one regime to the other.

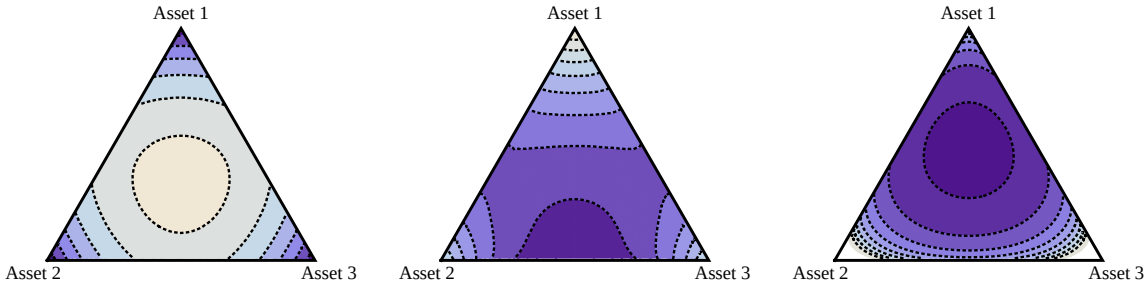

(a) Riskless rate (b) Asset 1's excess return (c) Asset 1's P/D

Figure 12: The riskless rate, and asset 1's excess return and price-dividend ratio.

The dependence of asset 1's price-dividend ratio on the state variable generates endogenous overreaction and underreaction to own-cashflow news, and positive or negative comovement in response to cashflow news of other assets. Figure 13a shows how asset 1's price responds to a 1% shock to its own dividend in different regions of the simplex. The contours indicate price increases of $0.5\%, 0.6\%, \ldots, 1.2\%$. The thick dashed contour indicates points at which the price increases by exactly 1%, i.e. at which valuation ratios remain constant. When asset 1 is large—above this contour—it overreacts to own-cashflow news. When it is small, it underreacts to cashflow news, particularly in the supercritical regime in which its price-dividend ratio declines rapidly as its dividend share increases.

Figure 13b shows how comovement arises, and specifically how asset 2's price responds to the 1% dividend shock to asset 1 (though because the calibration is symmetric, the figure can be used to work out how any of the three assets responds to any other). The contours indicate price increases of $-0.3\%, -0.2\%, \ldots, 0.7\%$. The thick dashed contour indicates points at which asset 2's price does not respond to a dividend shock for asset 1. If asset 1 is sufficiently large—at points above the contour—asset 2's price increases in response to good news for asset 1, i.e. there is positive comovement. If asset 1 is small, though, asset 2's price moves in the opposite direction following a shock to asset 1's dividend. This negative

comovement effect is strongest towards the bottom right corner of the simplex, where asset 2 is itself small and hence in its own supercritical regime.

Figure 13c puts everything together, plotting the correlation between the returns of assets 1 and 2. This is the correlation due to the Brownian component of the assets' returns, as would be calculated during normal times. The contours indicate correlations of 0% (the thick dashed contour), 10%, 20%, ..., 70%. If both assets 1 and 2 are very small, at the bottom right of the simplex, they are positively correlated with one another. This is not because they comove in response to each other's dividend shocks—on the contrary, Figure 13b shows that they comove negatively in response to each other's shocks—but because they both comove strongly with the dominant asset 3. As asset 3 becomes less dominant this second effect weakens, and we move into a region in which the correlation between assets 1 and 2 is negative, reaching a minimum of about -7%. In the middle of the figure, where all three assets have the same size, assets 1 and 2 have positive correlation. This is intuitive: the riskless rate attains its maximum at the center of the figure, so is constant near it, to first order. On the other hand, dividend shocks *do* have first order effects on risk premia in the familiar way. Thus a positive dividend shock for asset 1 drives down asset 2's share, depressing its required risk premium and leading to an appreciation in its valuation ratio, and hence to positive comovement. The same logic applies, *mutatis mutandis*, in the middle of the left-hand edge. Finally, if either asset 1 or asset 2 is dominant, the correlation is highest of all, rising above 70%. In this regime, the risk premium effect continues to operate, but there are now riskless rate effects that pull in opposite directions. Without loss of generality, suppose that asset 1 is large. Positive dividend news for asset 1 makes the world more unbalanced, driving the riskless rate down and amplifying the positive comovement of asset 2. On the other hand, positive dividend news for asset 2 pushes the riskless rate up, leading to *negative* comovement of asset 1. The first effect is quantitatively more important, however, so the overall result is that the correlation is highest of all when one of the two assets is dominant.

Using the information in Figures 13a and 13b, the simplex can be divided into three regions: if asset 1 is sufficiently dominant, it overreacts to own-cashflow news, and other assets comove positively with it; at the other extreme, if asset 1 is sufficiently small, it underreacts to own-cashflow news, and other assets comove negatively; in between, asset 1 underreacts to own-cashflow news and other assets comove positively with it. This last regime applies when all three assets are the same size, in the middle of the simplex, where the riskless rate is constant to first order.

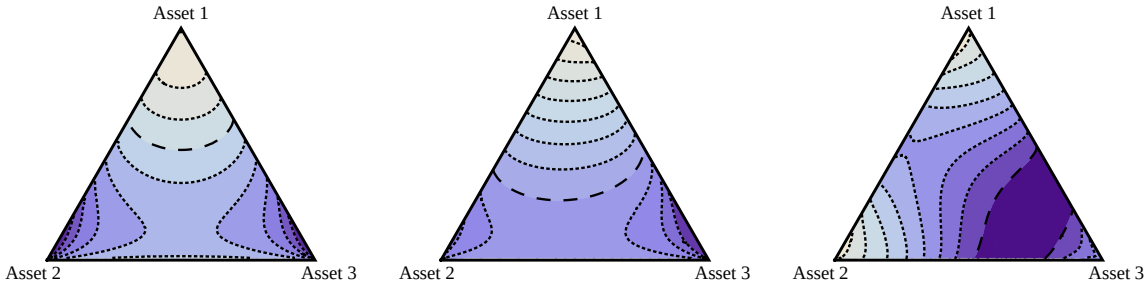

(a) Asset 1's response (b) Asset 2's response (c) Correlation in returns

Figure 13: The response of assets 1 and 2 to a shock to asset 1's dividend, and the correlation between the returns of assets 1 and 2. Asset 1 overreacts (underreacts) at points above (below) the dashed line in panel (a). Asset 2 comoves positively (negatively) at points above (below) the dashed line in panel (b). Correlation is negative in the dark band in panel (c), and positive elsewhere.

It is natural to ask what happens for larger N. How large must asset 1 be for other assets to comove with it? And how large must it be to overreact to its own cashflow news? In the $N = 2$ case, the issues of comovement and overreaction are intertwined: in a symmetric calibration, if an asset experiences overreaction when its share is larger than $\overline{s}$—where $\overline{s}$ is the point at which $P_1/D_1(s)$ achieves its minimum, $\overline{s} = 0.608$ in the present calibration—then other assets will comove with it when its share is larger than $1 - \overline{s}$.

	Comovement if...		Overreaction if...	
N	$s_1 \geq$	rel. size $\geq$	$s_1 \geq$	rel. size $\geq$
2	0.39	0.64	0.61	1.54
3	0.26	0.71	0.47	1.80
4	0.20	0.74	0.41	2.06
5	0.16	0.75	0.37	2.34
6	0.13	0.76	0.35	2.66

Table 2: Regions in which (positive) comovement and overreaction occur.

For $N = 3$ or larger, this tight link between overreaction and positive comovement is broken. Table 2 shows the corresponding results for N up to 6. In each case, I assume that asset 1 has dividend share s_1, and that all other assets are equally large, with dividend shares $(1 - s_1)/(N - 1)$. The column labelled "rel. size" shows the ratio of asset 1's dividend

share to the dividend share of (any) one of the other assets, i.e. $(N-1)s_1/(1-s_1)$. We have already seen that positive comovement and underreaction are the norm at the center of the state space. Indeed, positive comovement can occur even if asset 1 is significantly smaller than all the other assets. On the other hand, for an asset to overreact it must be significantly larger than all the other assets, and the relative amount by which it must be larger increases fairly rapidly with N.

Different calibrations deliver very similar results. In the no-jump calibration the critical values of s_1 are within 0.01 of those reported in Table 2. The same is true if we introduce correlation between dividends in such a way that that consumption volatility in the middle, where all assets have equal share, is held constant as N increases. On the other hand, the critical values at which comovement and overreaction take place *are* sensitive to γ. Lower γ reduces the variability of the riskless rate by more than it reduces the variability of risk premia, so underreaction and positive comovement occur over more of the simplex.

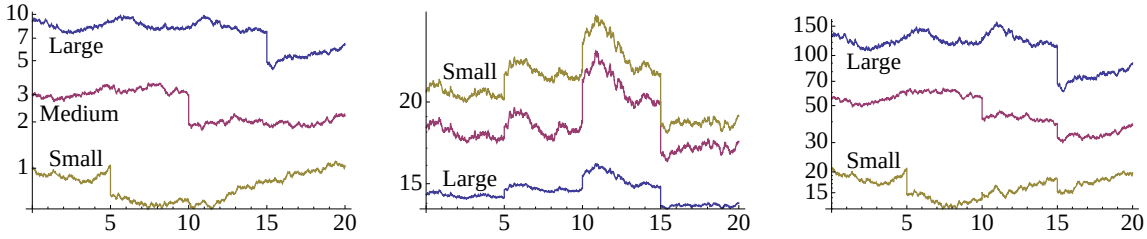

(a) Dividends (b) Price-dividend ratios (c) Prices

Figure 14: A 20-year sample path with initial dividends in proportions 9:3:1.

To make things more vivid, Figure 14 shows a 20-year sample path realization in the three-asset example, starting from a state of the world in which the assets have dividends of 9, 3, and 1 respectively. There are three disasters of equal severity over the sample period, one for each asset. These disasters provide a particularly clean illustration of the mechanism, since they isolate the effect of a dividend shock to a single asset. When the small asset experiences its dividend disaster, its own price drops sharply, though it underreacts since its price-dividend ratio increases. The medium and large assets comove negatively, and hence experience modest *upward* price jumps. When the medium-sized asset has a disaster, the same qualitative features occur, though with more quantitative impact than in the case of the small asset disaster. When the large asset has a disaster, all the assets comove positively, and experience large downward price jumps.

Figure 15 plots realized return correlations over the sample path, using 1-year rolling

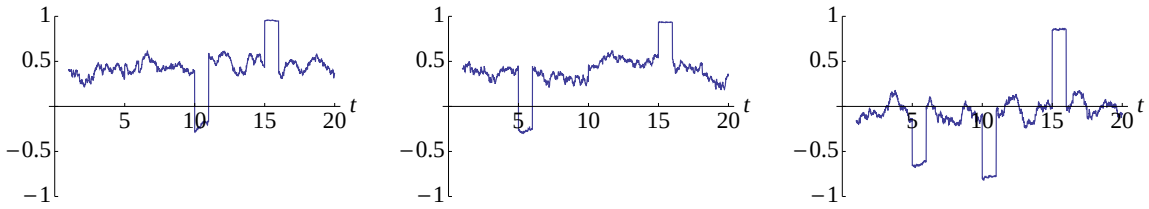

(a) Between large and medium (b) Between large and small (c) Between medium and small

Figure 15: Realized daily return correlations calculated from rolling 1-year horizons.

windows. The return correlation between large and medium, and between large and small, is on the order of 0.5 in normal times. In each case, this is because the positive comovement associated with shocks to the larger asset's dividend outweighs the negative comovement associated with shocks to the smaller asset's dividend. When the smaller asset experiences a disaster, however, the negative comovement comes to the fore, and we see the correlation jump down below zero. When the larger asset experiences a disaster, both the other assets move with it, and correlations spike close to one. Finally, the correlation between the medium and small assets is close to zero in normal times due to two offsetting effects: the two assets experience negative comovement in response to each other's cashflow shocks, but comove in response to the large asset's shocks. The former effect dominates when either the small or medium asset experiences a disaster, so correlations jump below zero; and the latter effect dominates when the large asset experiences a disaster, so correlations jump up. Such spikes in correlations are a familiar feature of the data, and here they arise in an example in which the correlation in *fundamentals* is constant—at zero—at all times.

4 Conclusion

This paper generalizes the model of Cochrane, Longstaff and Santa-Clara (2008) in three directions: it allows for power utility (rather than log), for dividends to follow exponential Lévy processes (rather than geometric Brownian motions), and for multiple assets (rather than just two). Each of these directions introduces interesting new types of behavior. Once risk aversion is higher than one, the CAPM fails, and the concern expressed by Cochrane, Longstaff and Santa-Clara that "the magnitudes are small" is lessened, because many of the quantities of interest increase faster than linearly in γ. When we allow for jumps, we step outside the familiar framework in which the ICAPM and consumption-CAPM hold. The riskless rate and equity premium puzzles can be avoided; more interestingly, jumps

spread across assets, and thereby provide a new channel for high risk premia even in assets that are not themselves subject to jumps in fundamentals. With more than two assets, we can untangle effects that cannot be separated when $N = 2$. For example, comovement and overreaction are two sides of the same coin when $N = 2$, but not when $N > 2$. It also becomes possible to differentiate between assets on both the size and value dimension; I explore this possibility in the online appendix. Jumps and multiple assets also interact in an interesting way, leading to spikes in correlations in both directions, as comovement effects that would be blurred together in Brownian-motion-driven models are isolated at the instant of a jump.

The solution method presented here is very different to that of Cochrane, Longstaff and Santa-Clara (2008). Their approach relies in part on an inspired guess-and-verify solution to an ODE, and in part on a series of miraculous identities between integrals. An unmotivated identity does occur at one point in this paper—in Step 3 of Appendix A.4, where I derive the closed form for the Brownian motion case—but in other respects my approach is (in a good sense) more *mechanical* and therefore more amenable to generalization. For example, Martin (2010) allows for imperfect substitution between the goods produced by the two trees, so that terms-of-trade effects enter the picture, and Chen and Joslin (2011) show how to handle the case with non-i.i.d. dividend growth. In a different direction, the approach taken here can be adapted to compute asset price behavior in an economy with two agents with differing risk aversion and one tree that is potentially subject to jumps, generalizing Wang (1996) and Longstaff and Wang (2008) (and closely related to Dumas (1989)); or to solve for asset prices with two trees and two agents with differing risk aversion.

There are two particularly obvious areas to work on. The riskless rate fluctuates significantly in the model. If the model could be generalized from power utility to Epstein-Zin (1989) preferences then this riskless rate variation could be dampened by letting the elasticity of intertemporal substitution exceed $1/\gamma$. An alternative view—which calls for a more ambitious extension of the model, allowing at the very least for goods to be stored over time—is that the riskless rate is stable not for reasons related to preferences, but for reasons related to technologies. In each case, it is likely that the effect of reducing riskless rate variation would be to enlarge the region in which underreaction and positive comovement take place. A second question is whether the N-asset integral formulas can be solved explicitly in special cases. It is desirable to try to do so because these formulas are subject to the curse of dimensionality, so become computationally intractable as N increases.

5 Bibliography

Andrews, G. E., Askey, R., and R. Roy (1999), *Special Functions*, Cambridge University Press, UK.

Barro, R. J. (2006), "Rare Disasters and Asset Markets in the Twentieth Century," *Quarterly Journal of Economics*, 121:3:823–866.

Brainard, W. C. and J. Tobin (1968), "Pitfalls in Financial Model Building," *American Economic Review*, 58:2:99–122.

Breeden, D. T. (1979), "An Intertemporal Asset Pricing Model with Stochastic Consumption and Investment Opportunities," *Journal of Financial Economics*, 7:265–296.

Campbell, J. Y. and J. Mei (1993), "Where do Betas Come From? Asset Price Dynamics and the Sources of Systematic Risk," *Review of Financial Studies*, 6:3:567–592.

Campbell, J. Y., C. Polk, and T. Vuolteenaho (2010), "Growth or Glamour? Fundamentals and Systematic Risk in Stock Returns," *Review of Financial Studies*, 23:1:305–344.

Campbell, J. Y. and T. Vuolteenaho (2004), "Bad Beta, Good Beta," *American Economic Review*, 94:5:1249–1275.

Chen, H., and S. Joslin (2011), "Generalized Transform Analysis of Affine Processes and Applications in Finance," working paper.

Cochrane, J. H. (2005), *Asset Pricing*, revised ed., Princeton University Press, Princeton, NJ.

Cochrane, J. H., Longstaff, F. A., and P. Santa-Clara (2008), "Two Trees," *Review of Financial Studies*, 21:1:347–385.

Cont, R. and P. Tankov (2004), *Financial Modelling with Jump Processes*, Chapman & Hall/CRC, Boca Raton, FL.

Dumas, B. (1989), "Two-Person Dynamic Equilibrium in the Capital Market," *Review of Financial Studies*, 2:2:157–188.

Dumas, B. (1992), "Dynamic Equilibrium and the Real Exchange Rate in a Spatially Separated World," *Review of Financial Studies*, 5:2:153–180.

Epstein, L., and S. Zin (1989), "Substitution, Risk Aversion, and the Temporal Behavior of Consumption and Asset Returns: A Theoretical Framework," *Econometrica*, 57:937–969.

Forbes, K. J. and R. Rigobon (2002), "No Contagion, Only Interdependence: Measuring Stock Market Comovements," *Journal of Finance*, 57:5:2223–2261.

Gollier, C. (2002), "Discounting an Uncertain Future," *Journal of Public Economics*, 85:149–166.

Longstaff, F. A., and J. Wang (2008), "Asset Pricing and the Credit Market," working paper.

Lucas, R. E. (1978), "Asset Prices in an Exchange Economy," *Econometrica*, 46:6:1429–1445.

Lucas, R. E. (1987), *Models of Business Cycles*, Basil Blackwell, Oxford, UK.

Martin, I. W. R. (2008), "Consumption-Based Asset Pricing with Higher Cumulants," working paper.

Martin, I. W. R. (2009), "The Valuation of Long-Dated Assets," working paper.

Mehra, R. and E. C. Prescott (1985), "The Equity Premium: A Puzzle," *Journal of Monetary Economics*, 15:145–161.

Menzly, L., Santos, T., and P. Veronesi (2004), "Understanding Predictability," *Journal of Political Economy*, 112:1:1–47.

Merton, R. C. (1973), "An Intertemporal Capital Asset Pricing Model," *Econometrica*, 41:5:867–887.

Pástor, L. and P. Veronesi (2003), "Stock Valuation and Learning about Profitability," *Journal of Finance*, 58:5:1749–1789.

Pástor, L. and P. Veronesi (2006), "Was there a Nasdaq Bubble in the Late 1990s?" *Journal of Financial Economics*, 81:61–100.

Pavlova, A. and R. Rigobon (2007), "Asset Prices and Exchange Rates," *Review of Financial Studies*, 20:4:1139–1181.

Rietz, T. A. (1988), "The Equity Premium: A Solution," *Journal of Monetary Economics*, 22:117–131.

Santos, T. and P. Veronesi (2006), "Labor Income and Predictable Stock Returns," *Review of Financial Studies*, 19:1:1–44.

Shiller, R. J. (1989), "Comovements in Stock Prices and Comovements in Dividends," *Journal of Finance*, 44:3:719–729.

Slater, L. J. (1966), *Generalized Hypergeometric Functions*, Cambridge University Press, UK.

Wang, J. (1996), "The Term Structure of Interest Rates in a Pure Exchange Economy with Heterogeneous Investors," *Journal of Financial Economics*, 41:75–110.

Weitzman, M. L. (1998), "Why the Far-Distant Future Should Be Discounted At Its Lowest Possible Rate," *Journal of Environmental Economics and Management*, 36:201–208.

A The two-asset case

A.1 The expectation

This section contains a calculation used in the proof of Proposition 1. The goal is to evaluate

$$E \equiv \mathbb{E}\left(\frac{e^{\alpha_1\widetilde{y}_{1t}+\alpha_2\widetilde{y}_{2t}}}{\left[e^{y_{10}+\widetilde{y}_{1t}}+e^{y_{20}+\widetilde{y}_{2t}}\right]^{\gamma}}\right) = e^{-\gamma/2(y_{10}+y_{20})}\cdot\mathbb{E}\left(\frac{e^{(\alpha_1-\gamma/2)\widetilde{y}_{1t}+(\alpha_2-\gamma/2)\widetilde{y}_{2t}}}{\left[2\cosh((y_{20}-y_{10}+\widetilde{y}_{2t}-\widetilde{y}_{1t})/2)\right]^{\gamma}}\right)$$

for general $\alpha_1, \alpha_2, \gamma > 0$. A word or two is in order to explain why it is natural to rearrange E like this. First, with power utility, valuation ratios should be unaffected if all assets are scaled up in size proportionally, so it is natural to look for a state variable like $y_{20} - y_{10}$. Second, a function must decline fast towards zero as it tends to plus or minus infinity in order to possess a Fourier transform. Thus it is natural to reshape the term inside the expectation into an exponential term in $\widetilde{y}_{1t}$ and $\widetilde{y}_{2t}$, which is easy to handle with the CGF, and a term in $[1/\cosh(\cdot)]^{\gamma}$, which is well behaved under the Fourier transform. Specifically, $1/\left[2\cosh(u/2)\right]^{\gamma}$ has a Fourier transform, $\mathscr{F}_{\gamma}(z)$, that can be found in closed form for integer

$\gamma > 0$, and satisfies

$$\frac{1}{[2\cosh(u/2)]^\gamma} = \int_{-\infty}^{\infty} e^{iuz} \mathscr{F}_\gamma(z)\, dz. \tag{23}$$

We have, then,

$$\begin{aligned} E &= e^{-\gamma(y_{10}+y_{20})/2}\ \mathbb{E}\left[e^{(\alpha_1-\gamma/2)\widetilde{y}_{1t}+(\alpha_2-\gamma/2)\widetilde{y}_{2t}} \int_{-\infty}^{\infty} \mathscr{F}_\gamma(z) e^{iz(y_{20}-y_{10})} e^{iz(\widetilde{y}_{2t}-\widetilde{y}_{1t})}\, dz\right] \\ &= e^{-\gamma(y_{10}+y_{20})/2} \int_{-\infty}^{\infty} \mathscr{F}_\gamma(z) e^{iz(y_{20}-y_{10})} e^{\boldsymbol{c}(\alpha_1-\gamma/2-iz,\alpha_2-\gamma/2+iz)t} \cdot\, dz\,. \end{aligned} \tag{24}$$

By the Fourier inversion theorem, definition (23) implies that

$$\mathscr{F}_\gamma(z) = \frac{1}{2\pi}\int_{-\infty}^{\infty} \frac{e^{-iuz}}{(2\cosh(u/2))^\gamma}\, du = \frac{1}{2\pi}\int_0^1 t^{\gamma/2-iz}(1-t)^{\gamma/2+iz}\frac{dt}{t(1-t)},$$

using the substitution $u = \log[t/(1-t)]$. This is a Dirichlet surface integral that can be evaluated in terms of Γ-functions, giving (5): see Andrews, Askey and Roy (1999, p. 34).

An alternative representation of $\mathscr{F}_\gamma(z)$ will also be useful. By contour integration, one can show that $\mathscr{F}_1(z) = \frac{1}{2}\operatorname{sech}\pi z$ and $\mathscr{F}_2(z) = \frac{1}{2} z \operatorname{cosech}\pi z$. From these two facts, expression (5), and the fact that $\Gamma(x) = (x-1)\Gamma(x-1)$, we have, for positive integer γ,

$$\mathscr{F}_\gamma(z) = \begin{cases} \dfrac{z\ \operatorname{cosech}(\pi z)}{2(\gamma-1)!} \cdot \displaystyle\prod_{n=1}^{\gamma/2-1} \left(z^2+n^2\right) & \text{for even } \gamma\,, \\ \dfrac{\operatorname{sech}(\pi z)}{2(\gamma-1)!} \cdot \displaystyle\prod_{n=1}^{(\gamma-1)/2} \left(z^2+(n-1/2)^2\right) & \text{for odd } \gamma\,. \end{cases} \tag{25}$$

A.2 Expected returns and interest rates

Given a jump-diffusion $\boldsymbol{y}$, with $d\boldsymbol{y} = \boldsymbol{\mu}dt + \boldsymbol{A}d\boldsymbol{Z} + \boldsymbol{J}dN$, there is a simple formula for $\mathbb{E}\, d(e^{\boldsymbol{w}'\boldsymbol{y}})$, where $\boldsymbol{w}$ is a constant vector. First, define $x \equiv \boldsymbol{w}'\boldsymbol{y}$; then $dx = \boldsymbol{w}'\boldsymbol{\mu}dt + \boldsymbol{w}'\boldsymbol{A}d\boldsymbol{Z} + \boldsymbol{w}'\boldsymbol{J}dN$. We seek $\mathbb{E}\, d(e^x)$. By Itô's formula for jump-diffusions, we have

$$d(e^x) = e^x\left[\left(\boldsymbol{w}'\boldsymbol{\mu} + \frac{1}{2}\boldsymbol{w}'\boldsymbol{\Sigma}\boldsymbol{w}\right)dt + \boldsymbol{w}'\boldsymbol{A}d\boldsymbol{Z} + \left(e^{\boldsymbol{w}'\boldsymbol{J}}-1\right)dN\right]$$

where $\boldsymbol{\Sigma} \equiv \boldsymbol{A}\boldsymbol{A}'$; and so, after taking expectations,

$$\mathbb{E}\, d(e^{\boldsymbol{w}'\boldsymbol{y}}) = e^{\boldsymbol{w}'\boldsymbol{y}} \cdot \left[\boldsymbol{w}'\boldsymbol{\mu} + \frac{1}{2}\boldsymbol{w}'\boldsymbol{\Sigma}\boldsymbol{w} + \omega\left(\mathbb{E}\, e^{\boldsymbol{w}'\boldsymbol{J}} - 1\right)\right]dt = e^{\boldsymbol{w}'\boldsymbol{y}} \cdot \boldsymbol{c}(\boldsymbol{w})dt\,. \tag{26}$$

If $\boldsymbol{y}$ is a general Lévy process, this holds by Proposition 8.20 of Cont and Tankov (2004).

For convenience, I write, throughout this section,

$$h(z) \equiv \frac{\mathscr{F}_\gamma(z)}{\rho - \boldsymbol{c}(\alpha_1-\gamma/2-iz, \alpha_2-\gamma/2+iz)} \quad \text{and} \quad \binom{n}{m} \equiv \frac{n!}{m!(n-m)!}.$$

Introducing this notation,

$$\begin{aligned} P_{\boldsymbol{\alpha}} &= \int_{-\infty}^{\infty} h(z) \cdot (e^{y_{10}} + e^{y_{20}})^{\gamma} \, e^{(\alpha_1 - \gamma/2 - iz)y_{10} + (\alpha_2 - \gamma/2 + iz)y_{20}} \, dz \\ &= \sum_{m=0}^{\gamma} \binom{\gamma}{m} \int_{-\infty}^{\infty} h(z) \cdot e^{\boldsymbol{w}_m(z) \cdot \boldsymbol{y}} \, dz \,, \end{aligned} \tag{27}$$

where $\boldsymbol{w}_m(z) \equiv (\alpha_1 - \gamma/2 + m - iz, \alpha_2 + \gamma/2 - m + iz)'$. Using (26),

$$\mathbb{E}(dP_{\boldsymbol{\alpha}}) = \left\{ \sum_{m=0}^{\gamma} \binom{\gamma}{m} \int_{-\infty}^{\infty} h(z) \cdot e^{\boldsymbol{w}_m(z) \cdot \boldsymbol{y}} \boldsymbol{c}\left[\boldsymbol{w}_m(z)\right] \, dz \right\} \cdot dt.$$

Dividing by (27) and rearranging, the expected capital gain is given by the formula

$$\frac{\mathbb{E}\, dP_{\boldsymbol{\alpha}}}{P_{\boldsymbol{\alpha}}} = \frac{\displaystyle\sum_{m=0}^{\gamma} \binom{\gamma}{m} e^{-mu} \int_{-\infty}^{\infty} h(z) e^{iuz} \cdot \boldsymbol{c}(\boldsymbol{w}_m(z)) \, dz}{\displaystyle\sum_{m=0}^{\gamma} \binom{\gamma}{m} e^{-mu} \int_{-\infty}^{\infty} h(z) e^{iuz} \, dz} \cdot dt.$$

Now for interest rates. From the Euler equation, we have

$$B_T = \mathbb{E}\left[e^{-\rho T} \left(\frac{C_T}{C_0} \right)^{-\gamma} \right] = e^{-\rho T} C_0^{\gamma} \, \mathbb{E}\left[\frac{1}{(D_{1T} + D_{2T})^{\gamma}} \right].$$

Using the result of Appendix A.1, we find that

$$\begin{aligned} B_T &= e^{-\rho T} \, (e^{y_{10}} + e^{y_{20}})^{\gamma} \, e^{-\gamma(y_{10} + y_{20})/2} \int_{-\infty}^{\infty} e^{iz(y_{20} - y_{10})} \, \mathscr{F}_{\gamma}(z) e^{\boldsymbol{c}(-\gamma/2 - iz, -\gamma/2 + iz)T} \, dz \\ &= e^{-\rho T} \, [2\cosh(u/2)]^{\gamma} \int_{-\infty}^{\infty} \mathscr{F}_{\gamma}(z) e^{iuz} \cdot e^{\boldsymbol{c}(-\gamma/2 - iz, -\gamma/2 + iz)T} \, dz \,, \end{aligned}$$

from which (8) follows, and hence also (9), by l'Hôpital's rule.

The function $\rho - \boldsymbol{c}(-\gamma/2 - iz, -\gamma/2 + iz)$, considered as a function of $z \in \mathbb{C}$, has a stationary point on the imaginary axis. Call it $z^* = is^*$, where $s^* \in \mathbb{R}$; then s^* maximizes $\rho - \boldsymbol{c}(-\gamma/2 + s, -\gamma/2 - s)$. Poles of the integrand in (8) occur at the poles of $\mathscr{F}_{\gamma}(z)$: that is, at $\pm(\gamma/2)i, \pm(\gamma/2 + 1)i$, and so on. If $|s^*| < \gamma/2$ then the contour of integration in (8) (i.e. the real axis) can be deformed to pass through is^* without crossing a pole, and therefore without altering the value of the integral, by Cauchy's theorem. It follows that $\mathscr{Y}(\infty) = \rho - \boldsymbol{c}(-\gamma/2 + s^*, -\gamma/2 - s^*)$ by the method of steepest descent.

If $|s^*| \geq \gamma/2$, then deforming the contour of integration to pass through is^* requires a pole to be crossed, and hence a residue to be taken into account. This residue, rather than the precise location of is^*, turns out to dictate the behavior of the long end of the

yield curve. If $s^* > \gamma/2$, for example, the integral to be evaluated picks up an extra term proportional to $e^{-[\rho-\boldsymbol{c}(0,-\gamma)]T}$. Since $\rho-\boldsymbol{c}(-\gamma/2+s^*,-\gamma/2-s^*)$ is larger than $\rho-\boldsymbol{c}(0,-\gamma)$ by construction of s^*, the term in $e^{-[\rho-\boldsymbol{c}(-\gamma/2+s^*,-\gamma/2-s^*)]T}$ is irrelevant in the limit, and $\mathscr{Y}(\infty)=\rho-\boldsymbol{c}(0,-\gamma)$. Moreover, in this situation, concavity of $\rho-\boldsymbol{c}(-\gamma/2+s,-\gamma/2-s)$ implies that $\rho-\boldsymbol{c}(0,-\gamma)>\rho-\boldsymbol{c}(-\gamma/2+s,-\gamma/2-s)$ for all $s<\gamma/2$. An almost identical argument shows that if $s^*<-\gamma/2$, we have $\mathscr{Y}(\infty)=\rho-\boldsymbol{c}(-\gamma,0)$, and that in this situation $\rho-\boldsymbol{c}(-\gamma,0)>\rho-\boldsymbol{c}(-\gamma/2+s,-\gamma/2-s)$ for all $s>-\gamma/2$. Equation (10) follows.

A.3 Consequences of the finiteness condition

This section develops two consequences of the finiteness condition $\rho-\boldsymbol{c}(\alpha_1-\gamma/2,\alpha_2-\gamma/2)>0$, which is assumed to hold for the values of α_1 and α_2 discussed in Table 1.

Lemma 1. *For $z_1,z_2\in\mathbb{C}$, we have $\operatorname{Re}\boldsymbol{c}(z_1,z_2)\le\boldsymbol{c}(\operatorname{Re}z_1,\operatorname{Re}z_2)$. The inequality is strict if z_1 and z_2 have nonzero imaginary parts and $\widetilde{\boldsymbol{y}}_1$ has uncountable essential support.*

Proof. For any $z\in\mathbb{C}$, $\operatorname{Re}\log z=\log|z|$. It follows that $\operatorname{Re}\boldsymbol{c}(z_1,z_2)=\log\left|\mathbb{E}\,e^{z_1\widetilde{y}_{11}+z_2\widetilde{y}_{21}}\right|\le\log\mathbb{E}\left|e^{z_1\widetilde{y}_{11}+z_2\widetilde{y}_{21}}\right|=\log\mathbb{E}\,e^{\operatorname{Re}z_1\cdot\widetilde{y}_{11}+\operatorname{Re}z_2\cdot\widetilde{y}_{21}}=\boldsymbol{c}(\operatorname{Re}z_1,\operatorname{Re}z_2)$. The inequality is strict unless $e^{z_1\widetilde{y}_{11}+z_2\widetilde{y}_{21}}$ is real almost surely or imaginary almost surely, which is not the case if z_1 and z_2 have nonzero imaginary parts and $\widetilde{\boldsymbol{y}}_1$ has uncountable essential support. □

For $\widetilde{\boldsymbol{y}}_1$ to have uncountable essential support it is sufficient, but not necessary, that one of the dividend processes has a Brownian component or is subject to jumps witih continuous size distribution. The only remotely natural example in which the inequality in Lemma 1 is not strict is if log dividends follow a pure jump process with jumps of fixed size.

Lemma 2. *For all $z\in\mathbb{R}$, we have $\rho-Re\left[\boldsymbol{c}(\alpha_1-\gamma/2-iz,\alpha_2-\gamma/2+iz)\right]>0$.*

Proof. From Lemma 1, $\operatorname{Re}\boldsymbol{c}(\alpha_1-\gamma/2-iz,\alpha_2-\gamma/2+iz)\le\boldsymbol{c}(\alpha_1-\gamma/2,\alpha_2-\gamma/2)$, so $\rho-\operatorname{Re}\boldsymbol{c}(\alpha_1-\gamma/2-iz,\alpha_2-\gamma/2+iz)\ge\rho-\boldsymbol{c}(\alpha_1-\gamma/2,\alpha_2-\gamma/2)>0$. □

Definition 4. *Let f be a meromorphic function. A zero (or pole) of f is* minimal *if it lies in the upper half-plane and no other such zero (or pole) has smaller imaginary part.*

Lemma 2 shows that $\rho-\boldsymbol{c}(\alpha_1-\gamma/2-iz,\alpha_2-\gamma/2+iz)$ has no zeros on the real axis. The next result documents an important property of its minimal zero.

Lemma 3. *If $\widetilde{\boldsymbol{y}}_1$ has uncountable essential support, then the minimal zero of $\rho-\boldsymbol{c}(\alpha_1-\gamma/2-iz,\alpha_2-\gamma/2+iz)$, if it exists, is unique and lies on the imaginary axis.*

Proof. Let $p+qi$ be a minimal zero, and suppose (aiming for a contradiction) that $p \neq 0$. Lemma 1 applies with strict inequality, so $\rho - \boldsymbol{c}(\alpha_1 - \gamma/2 + q, \alpha_2 - \gamma/2 - q) < 0$. But then the finiteness condition and the intermediate value theorem imply that there exists $q_2 \in (0, q)$ such that $\rho - \boldsymbol{c}(\alpha_1 - \gamma/2 + q_2, \alpha_2 - \gamma/2 - q_2) = 0$. If so, $q_2 i$ is a zero with $q_2 < q$, so $p+qi$ is not minimal, giving the desired contradiction. □

A.4 The Brownian motion case

In the Brownian motion case, $\boldsymbol{c}(\theta_1, \theta_2) = \mu_1\theta_1 + \mu_2\theta_2 + \frac{1}{2}\sigma_{11}\theta_1^2 + \sigma_{12}\theta_1\theta_2 + \frac{1}{2}\sigma_{22}\theta_2^2$. There are two solutions to the equation $\rho - \boldsymbol{c}(\alpha_1 - \gamma/2 - iz, \alpha_2 - \gamma/2 + iz) = 0$, each of which lies on the imaginary axis. One—call it $\lambda_1 i$—lies in the upper half-plane; the other—call it $\lambda_2 i$—lies in the lower half-plane. We can rewrite $\rho - \boldsymbol{c}(\alpha_1 - \gamma/2 - iz, \alpha_2 - \gamma/2 + iz) = B(z - \lambda_1 i)(z - \lambda_2 i)$ for $B > 0, \lambda_1 > 0, \lambda_2 < 0$ given in the main text. The aim, then, is to evaluate

$$I \equiv \int_{-\infty}^{\infty} \frac{e^{iuz}\mathscr{F}_\gamma(z)}{B(z - \lambda_1 i)(z - \lambda_2 i)}\, dz\,, \tag{28}$$

in terms of which the price-dividend ratio is $P/D = [2\cosh(u/2)]^\gamma \cdot I$.

The proof of Proposition 4 is somewhat involved, so I have divided it into several steps. Step 1 starts from the assumption that the state variable u is positive and shows that the integral (28) can be calculated using the residue theorem. Steps 2 and 3 carry out these calculations and simplify. Step 4 extends the result to negative u.

Step 1. Let $u > 0$. Consider the case in which γ is even. Let $R_n \equiv n + 1/2$, where n is an integer. Define the large semicircle Ω_n to be the semicircle whose base lies along the real axis from $-R_n$ to R_n and which has a semicircular arc (ω_n) passing through the upper half-plane from R_n through $R_n i$ and back to $-R_n$. I will first show that

$$I = \lim_{n\to\infty} \int_{\Omega_n} \frac{e^{iuz}\mathscr{F}_\gamma(z)}{B(z - \lambda_1 i)(z - \lambda_2 i)}\, dz\,. \tag{29}$$

Then, from the residue theorem, it will follow that

$$I = 2\pi i \cdot \sum \operatorname{Res}\left\{ \frac{e^{iuz}\mathscr{F}_\gamma(z)}{B(z - \lambda_1 i)(z - \lambda_2 i)}; z_p \right\}, \tag{30}$$

where the sum is taken over all poles z_p in the upper half-plane.

The first step is to establish that (29) holds. The right-hand side is equal to

$$\lim_{n\to\infty} \underbrace{\int_{-R_n}^{R_n} \frac{e^{iuz}\mathscr{F}_\gamma(z)}{B(z - \lambda_1 i)(z - \lambda_2 i)}\, dz}_{I_n} + \underbrace{\int_{\omega_n} \frac{e^{iuz}\mathscr{F}_\gamma(z)}{B(z - \lambda_1 i)(z - \lambda_2 i)}\, dz}_{J_n}$$

The integral I_n tends to I as $n \to \infty$. The aim, then, is to establish that the second term J_n tends to zero as $n \to \infty$. Along the arc ω_n, we have $z = R_n e^{i\theta}$ where θ varies between 0 and π. At this point it is convenient to work with the representation of $\mathscr{F}_\gamma(z)$ of equation (25). Substituting from (25), we have

$$J_n = \int_0^\pi \frac{e^{iuR_n\cos\theta - uR_n\sin\theta}P(R_n e^{i\theta})}{Q(R_n e^{i\theta})\left(e^{\pi R_n(\cos\theta+i\sin\theta)} - e^{-\pi R_n(\cos\theta+i\sin\theta)}\right)} \cdot R_n i e^{i\theta}\, d\theta$$

with $P(\cdot)$ and $Q(\cdot)$ polynomials.

To show that J_n tends to zero as n tends to infinity, I separate the range of integration $[0,\pi]$ into two parts: $[\pi/2-\delta, \pi/2+\delta]$ and its complement in $[0,\pi]$. Here δ will be chosen to be extremely small. First, consider

$$\begin{aligned} J_n^{(1)} &\equiv \left| \int_{\pi/2-\delta}^{\pi/2+\delta} \frac{P(R_n e^{i\theta})e^{iuR_n\cos\theta - uR_n\sin\theta}R_n i e^{i\theta}}{Q(R_n e^{i\theta})\left(e^{\pi R_n(\cos\theta+i\sin\theta)} - e^{-\pi R_n(\cos\theta+i\sin\theta)}\right)}\, d\theta \right| \\ &\leq \int_{\pi/2-\delta}^{\pi/2+\delta} \left|\frac{P(R_n e^{i\theta})}{Q(R_n e^{i\theta})}\right| \frac{e^{-uR_n\sin\theta}R_n}{\left|e^{\pi R_n(\cos\theta+i\sin\theta)} - e^{-\pi R_n(\cos\theta+i\sin\theta)}\right|}\, d\theta \end{aligned}$$

Pick δ sufficiently small that

$$\left|e^{\pi R_n(\cos\theta+i\sin\theta)} - e^{-\pi R_n(\cos\theta+i\sin\theta)}\right| \geq 2-\varepsilon$$

for all $\theta \in [\pi/2-\delta, \pi/2+\delta]$; ε is some very small number close to but greater than zero. This is possible because the left-hand side is continuous, and equals 2 when $\theta = \pi/2$. Then,

$$J_n^{(1)} \leq \int_{\pi/2-\delta}^{\pi/2+\delta} \left|\frac{P(R_n e^{i\theta})}{Q(R_n e^{i\theta})}\right| \frac{e^{-uR_n\sin\theta}R_n}{2-\varepsilon}\, d\theta \tag{31}$$

Since (i) we can also ensure that δ is small enough that $\sin\theta \geq \varepsilon$ for θ in the range of integration; (ii) $|P(R_n e^{i\theta})| \leq P_2(R_n)$, where P_2 is the polynomial obtained by taking absolute values of the coefficients in P; (iii) $Q(R_n e^{i\theta})$ tends to infinity as R_n becomes large; and (iv) decaying exponentials decay faster than polynomials grow, in the sense that for any positive k and λ, $x^k e^{-\lambda x} \to 0$ as $x \to \infty$, $x \in \mathbb{R}$, we see, finally, that the right-hand side of (31), and hence $J_n^{(1)}$, tends to zero as $n \to \infty$.

It remains to be shown that

$$J_n^{(2)} \equiv \left| \int_{[0,\pi/2-\delta]\cup[\pi/2+\delta,\pi]} \frac{P(R_n e^{i\theta})e^{iuR_n\cos\theta - uR_n\sin\theta}R_n i e^{i\theta}}{Q(R_n e^{i\theta})\left(e^{\pi R_n(\cos\theta+i\sin\theta)} - e^{-\pi R_n(\cos\theta+i\sin\theta)}\right)}\, d\theta \right|$$

is zero in the limit. Since $\delta > 0$, for all θ in the range of integration we have that $|\cos\theta| \geq \zeta > 0$, for some small ζ. We have

$$J_n^{(2)} \leq \int_{[0,\pi/2-\delta]\cup[\pi/2+\delta,\pi]} \left|\frac{P(R_n e^{i\theta})}{Q(R_n e^{i\theta})}\right| \frac{e^{-uR_n\sin\theta}R_n}{\left|e^{\pi R_n(\cos\theta+i\sin\theta)} - e^{-\pi R_n(\cos\theta+i\sin\theta)}\right|}\, d\theta\,.$$

Now,

$$\begin{aligned}\left|e^{\pi R_n(\cos\theta+i\sin\theta)}-e^{-\pi R_n(\cos\theta+i\sin\theta)}\right| &\geq \left|\left|e^{\pi R_n(\cos\theta+i\sin\theta)}\right|-\left|e^{-\pi R_n(\cos\theta+i\sin\theta)}\right|\right| \\ &= e^{\pi R_n|\cos\theta|}-e^{-\pi R_n|\cos\theta|} \\ &\geq e^{\pi R_n\zeta}-e^{-\pi R_n\zeta}\end{aligned}$$

for all θ in the range of integration. So,

$$\begin{aligned}J_n^{(2)} &\leq \int_{[0,\pi/2-\delta]\cup[\pi/2+\delta,\pi]}\left|\frac{P(R_ne^{i\theta})}{Q(R_ne^{i\theta})}\right|\frac{e^{-uR_n\sin\theta}R_n}{e^{\pi R_n\zeta}-e^{-\pi R_n\zeta}}\,d\theta \\ &\leq \int_{[0,\pi/2-\delta]\cup[\pi/2+\delta,\pi]}\left|\frac{P(R_ne^{i\theta})}{Q(R_ne^{i\theta})}\right|\frac{R_n}{e^{\pi R_n\zeta}-e^{-\pi R_n\zeta}}\,d\theta\end{aligned}$$

which tends to zero as n tends to infinity.

The case of γ odd is almost identical. The only important difference is that we take $R_n = n$ (as opposed to $n+1/2$) before allowing n to go to infinity. The reason for doing so is that we must take care to avoid the poles of $\mathscr{F}_\gamma(z)$ on the imaginary axis.

Step 2. From now on, I revert to the definition of $\mathscr{F}_\gamma(z)$ given in (5). The integrand is

$$\frac{e^{iuz}\Gamma(\gamma/2-iz)\Gamma(\gamma/2+iz)}{2\pi\cdot B\cdot\Gamma(\gamma)\cdot(z-\lambda_1 i)(z-\lambda_2 i)}\,, \tag{32}$$

which has poles in the upper half-plane at $\lambda_1 i$ and at points z such that $\gamma/2+iz=-n$ for integers $n\geq 0$, since the Γ-function has poles at the negative integers and zero. Combining the two, (32) has poles at $\lambda_1 i$ and at $(n+\gamma/2)i$ for $n\geq 0$.

We can calculate the residue of (32) at $z=\lambda_1 i$ directly, using the fact that if $f(z)=g(z)/h(z)$ has a pole at a, and $g(a)\neq 0$, $h(a)=0$, and $h'(a)\neq 0$, then $\operatorname{Res}\{f(z);a\}=g(a)/h'(a)$. The residue at $\lambda_1 i$ is therefore

$$\frac{e^{-\lambda_1 u}\Gamma(\gamma/2+\lambda_1)\Gamma(\gamma/2-\lambda_1)}{2\pi i\cdot B\cdot\Gamma(\gamma)\cdot(\lambda_1-\lambda_2)}\,. \tag{33}$$

For integer $n\geq 0$, $\Gamma(z)$ has residue $(-1)^n/n!$ at $z=-n$, so the residue of (32) at $(n+\gamma/2)i$ is

$$\frac{-e^{-u(n+\gamma/2)}\cdot\Gamma(\gamma+n)\cdot\frac{(-1)^n}{n!}}{2\pi i\cdot B\cdot\Gamma(\gamma)\cdot(n+\gamma/2-\lambda_1)(n+\gamma/2-\lambda_2)} \tag{34}$$

Substituting (33) and (34) into (30), we find

$$I=\frac{e^{-\lambda_1 u}\Gamma(\gamma/2+\lambda_1)\Gamma(\gamma/2-\lambda_1)}{B\cdot\Gamma(\gamma)\cdot(\lambda_1-\lambda_2)}-e^{-\gamma u/2}\sum_{n=0}^{\infty}\frac{(-e^{-u})^n\cdot\Gamma(\gamma+n)\cdot\frac{1}{n!}}{B\cdot\Gamma(\gamma)\cdot(n+\gamma/2-\lambda_1)(n+\gamma/2-\lambda_2)}$$

Since $|-e^{-u}|<1$ under the assumption that $u>0$, which for the time being is still maintained, we can use the series definition of Gauss's hypergeometric function (11), together with the fact that $\Gamma(\gamma+n)/\Gamma(\gamma)=\gamma(\gamma+1)\cdots(\gamma+n-1)$, to obtain

$$\begin{aligned} I &= \frac{e^{-\lambda_1 u}}{B(\lambda_1-\lambda_2)}\frac{\Gamma(\gamma/2-\lambda_1)\Gamma(\gamma/2+\lambda_1)}{\Gamma(\gamma)}+ \\ &\quad+\frac{e^{-\gamma u/2}}{B(\lambda_1-\lambda_2)}\left[\frac{1}{\gamma/2-\lambda_2}F\left(\gamma,\gamma/2-\lambda_2;1+\gamma/2-\lambda_2;-e^{-u}\right)-\right. \\ &\qquad\left.-\frac{1}{\gamma/2-\lambda_1}F\left(\gamma,\gamma/2-\lambda_1;1+\gamma/2-\lambda_1;-e^{-u}\right)\right] \end{aligned} \tag{35}$$

Step 3. A further simplification follows from the fact that

$$\begin{aligned} e^{-\lambda_1 u}\frac{\Gamma(\gamma/2-\lambda_1)\Gamma(\gamma/2+\lambda_1)}{\Gamma(\gamma)} &= \frac{e^{\gamma u/2}}{\gamma/2+\lambda_1}F\left(\gamma,\gamma/2+\lambda_1;1+\gamma/2+\lambda_1;-e^{u}\right)+ \\ &\quad+\frac{e^{-\gamma u/2}}{\gamma/2-\lambda_1}F\left(\gamma,\gamma/2-\lambda_1;1+\gamma/2-\lambda_1;-e^{-u}\right), \end{aligned}$$

which follows from equation (1.8.1.11) of Slater (1966, pp. 35–36). Using this in (35),

$$\begin{aligned} I &= \frac{1}{B(\lambda_1-\lambda_2)}\left[\frac{e^{\gamma u/2}}{\gamma/2+\lambda_1}F\left(\gamma,\gamma/2+\lambda_1;1+\gamma/2+\lambda_1;-e^{u}\right)+\right. \\ &\qquad\left.+\frac{e^{-\gamma u/2}}{\gamma/2-\lambda_2}F\left(\gamma,\gamma/2-\lambda_2;1+\gamma/2-\lambda_2;-e^{-u}\right)\right]. \end{aligned}$$

It follows that

$$\begin{aligned} P/D_1(u) &= \frac{[2\cosh(u/2)]^{\gamma}}{B(\lambda_1-\lambda_2)}\left[\frac{e^{\gamma u/2}}{\gamma/2+\lambda_1}F\left(\gamma,\gamma/2+\lambda_1;1+\gamma/2+\lambda_1;-e^{u}\right)+\right. \\ &\qquad\left.+\frac{e^{-\gamma u/2}}{\gamma/2-\lambda_2}F\left(\gamma,\gamma/2-\lambda_2;1+\gamma/2-\lambda_2;-e^{-u}\right)\right]; \end{aligned} \tag{36}$$

thus far, however, the derivation is valid only under the assumption that $u>0$.

Step 4. Suppose, now, that $u<0$. Take the complex conjugate of equation (28). Doing so is equivalent to reframing the problem with (u,λ_1,λ_2) replaced by $(-u,-\lambda_2,-\lambda_1)$. Since $-u>0,-\lambda_2>0$, and $-\lambda_1<0$, the method of steps 1–4 applies unchanged. Since the formula (36) is invariant under $(-u,-\lambda_2,-\lambda_1)\mapsto(u,\lambda_1,\lambda_2)$, we can conclude that it is valid for all u. Substituting $u\mapsto\log(1-s)/s$ delivers (12).

Step 5. Straightforward algebra gives the values of B, λ_1, and λ_2 in terms of the fundamental parameters. Since $\boldsymbol{c}(\theta_1,\theta_2)=\mu_1\theta_1+\mu_2\theta_2+\frac{1}{2}\sigma_{11}\theta_1^2+\sigma_{12}\theta_1\theta_2+\frac{1}{2}\sigma_{22}\theta_2^2$,

$$\rho-\boldsymbol{c}(\alpha_1-\gamma/2-iz,\alpha_2-\gamma/2+iz)=\frac{1}{2}X^2z^2+iYz+\frac{1}{2}Z^2, \tag{37}$$

where X^2, Y, and Z^2 are defined in the main text. I have chosen to write X^2 and Z^2 to emphasize that these two quantities are positive: the first because it is the variance of $y_{21} - y_{11}$, the second because of the finiteness conditions, after setting $v = 0$ in (37).

A.5 Small asset asymptotics

From (4), the small asset's price-dividend ratio in the limit can be rewritten

$$P/D_1 = \lim_{u\to\infty} \frac{\displaystyle\int_{-\infty}^{\infty} \frac{e^{iuz}\mathscr{F}_\gamma(z)}{\rho - \boldsymbol{c}(1-\gamma/2-iz, -\gamma/2+iz)}\,dz}{\displaystyle\int_{-\infty}^{\infty} e^{iuz}\mathscr{F}_\gamma(z)\,dz}\,. \tag{38}$$

By the Riemann-Lebesgue lemma, both the numerator and denominator on the right-hand side of (38) tend to zero in the limit as u tends to infinity. What happens to their ratio? This section shows how to calculate limiting price-dividend ratio, riskless rate and excess returns in the small-asset case. For clarity, I work through the price-dividend ratio in detail; the same approach applies to the riskless rate and to expected returns. At the end of the section, I discuss the corresponding calculations for the large asset.

Step 1. Consider the integral which makes up the numerator of (38),

$$I \equiv \int_{-\infty}^{\infty} \frac{e^{iuz}\mathscr{F}_\gamma(z)}{\rho - \boldsymbol{c}(1-\gamma/2-iz, -\gamma/2+iz)}\,dz\,.$$

If log dividends are drifting Brownian motions, Appendix A.4 showed that this integral could be approached by summing all residues in the upper half-plane. The aim here is to show that the *asymptotic* behavior of this integral in the general case is determined only by the minimal residue as discussed in the main text. To show this, I integrate around a contour which avoids all poles except for the minimal pole. Either the minimal pole occurs at the minimal zero of $\rho - \boldsymbol{c}(1-\gamma/2-iz, -\gamma/2+iz)$, so lies on the imaginary axis by Lemma 3, or the minimal pole occurs at the minimal pole of $\mathscr{F}_\gamma(z)$, i.e. at $i\gamma/2$. In either case, the minimal pole occurs at some point mi, where $m > 0$ is real. See Figure 10.

Let $\square_N$ denote the rectangle in the complex plane with corners at $-N$, N, $N+(m+\varepsilon)i$ and $-N+(m+\varepsilon)i$. Since the integrand is meromorphic, all poles are isolated, so $\varepsilon > 0$ can be chosen to be sufficiently small that the rectangle $\square_N$ only contains the pole at mi. By

the residue theorem, we have

$$\begin{aligned} J &\equiv \int_{\square_N} \frac{e^{iuz}\mathscr{F}_\gamma(z)}{\rho - \boldsymbol{c}(1-\gamma/2-iz,-\gamma/2+iz)}\,dz \\ &= 2\pi i \text{ Res}\left\{\frac{e^{iuz}\mathscr{F}_\gamma(z)}{\rho - \boldsymbol{c}(1-\gamma/2-iz,-\gamma/2+iz)}; mi\right\}. \end{aligned}$$

On the other hand, we can also decompose the integral into four pieces:

$$\begin{aligned} J &= \int_{-N}^{N} \frac{e^{iuz}\mathscr{F}_\gamma(z)}{\rho - \boldsymbol{c}(1-\gamma/2-iz,-\gamma/2+iz)}\,dz + \int_0^{m+\varepsilon} \frac{e^{iu(N+iz)}\mathscr{F}_\gamma(N+iz)}{\rho-\boldsymbol{c}(\ldots)}\,i\,dz + \\ &\quad + \int_N^{-N} \frac{e^{iu(z+(m+\varepsilon)i)}\mathscr{F}_\gamma(z+(m+\varepsilon)i)}{\rho-\boldsymbol{c}(\ldots)}\,dz + \int_{m+\varepsilon}^{0} \frac{e^{iu(-N+iz)}\mathscr{F}_\gamma(-N+iz)}{\rho-\boldsymbol{c}(\ldots)}\,i\,dz \\ &\equiv J_1 + J_2 + J_3 + J_4 \end{aligned}$$

I now show that J_2, J_3, and J_4 tend to zero as N and u tend to infinity. Consider J_2. Since the range of integration is a closed and bounded interval, the function $|\rho - \boldsymbol{c}(\ldots)|$ attains its maximum and minimum on the range. Since the function has no zeros on the interval, we can write $|\rho - \boldsymbol{c}(\ldots)| \geq \delta_1 > 0$ for all z in the range of integration. We have

$$\begin{aligned} |J_2| &\leq \int_0^{m+\varepsilon} \left|\frac{e^{iu(N+iz)}\mathscr{F}_\gamma(N+iz)}{\rho-\boldsymbol{c}(\ldots)}\,i\right| dz \\ &= \int_0^{m+\varepsilon} \frac{e^{-uz}\,|\mathscr{F}_\gamma(N+iz)|}{|\rho-\boldsymbol{c}(\ldots)|}\,dz \\ &\leq \frac{1}{\delta_1}\int_0^{m+\varepsilon} |\mathscr{F}_\gamma(N+iz)|\,dz \\ &\to 0 \end{aligned}$$

as N tends to infinity because $|\mathscr{F}_\gamma(N+iz)|$ converges to zero uniformly over z in the range of integration. An almost identical argument shows that $|J_4| \to 0$ as $N \to \infty$.

Now consider J_3. Set $\delta_2 = |\rho - \boldsymbol{c}(1-\gamma/2+m+\varepsilon, -\gamma/2-m-\varepsilon)| > 0$. Using the results of Appendix A.3, $|\rho - \boldsymbol{c}(\ldots)| \geq \delta_2$ for all z in the range of integration, so

$$\begin{aligned} |J_3| &\leq \int_{-N}^{N} \frac{e^{-(m+\varepsilon)u}\,|\mathscr{F}_\gamma(z+(m+\varepsilon)i)|}{|\rho-\boldsymbol{c}(\ldots)|}\,dz \\ &\leq e^{-u(m+\varepsilon)}\cdot\frac{1}{\delta_2}\int_{-N}^{N} |\mathscr{F}_\gamma(z+(m+\varepsilon)i)|\,dz \\ &\to e^{-u(m+\varepsilon)}\cdot X/\delta_2 \end{aligned}$$

where X is the (finite) limit of the integral $\int_{-N}^{N} |\mathscr{F}_\gamma(z+(m+\varepsilon)i)|\,dz$ as N tends to infinity. (X is finite because $\mathscr{F}_\gamma(z+(m+\varepsilon)i)$ decays to zero exponentially fast as $z \to \pm\infty$.)

By the residue theorem, $J_1 + J_2 + J_3 + J_4 = 2\pi i \times$ residue at $mi = O(e^{-mu})$. As N goes to infinity, J_2 and J_4 go to zero, J_1 tends to I and J_3 tends to $e^{-u(m+\varepsilon)}X$; so $I + e^{-u(m+\varepsilon)}X = 2\pi i \times$ residue at $mi = O(e^{-mu})$. In the limit as $u \to \infty$, $e^{-u(m+\varepsilon)}X$ is exponentially smaller than e^{-mu}, so

$$I \sim 2\pi i \text{ Res}\left\{\frac{e^{iuz}\mathscr{F}_\gamma(z)}{\rho - \boldsymbol{c}(1-\gamma/2-iz,-\gamma/2+iz)}; mi\right\} :$$

the asymptotic behavior of I is dictated by the residue closest to the real line.

Essentially identical arguments can be made to show that the other relevant integrals are asymptotically equivalent to $2\pi i$ times the minimal residue of the relevant integrand; they are omitted to prevent an already complicated argument becoming totally unreadable.

Step 2. (i) In the price-dividend ratio case, we have to evaluate

$$\lim_{u\to\infty} P/D(u) = \lim_{u\to\infty} \frac{\displaystyle\int_{-\infty}^{\infty} \frac{e^{iuz}\mathscr{F}_\gamma(z)}{\rho - \boldsymbol{c}(1-\gamma/2-iz,-\gamma/2+iz)}\,dz}{\displaystyle\int_{-\infty}^{\infty} e^{iuz}\mathscr{F}_\gamma(z)\,dz} \equiv \lim_{u\to\infty}\frac{I_n}{I_d}\,. \tag{39}$$

We have seen that I_n and I_d are asymptotically equivalent to $2\pi i$ times the residue at the pole (of the relevant integrand) with smallest imaginary part. I will refer to the pole (or zero) with least positive imaginary part as the *minimal* pole (or zero).

Consider, then, the more complicated integral I_n. The integrand has a pole at $i\gamma/2$ due to a singularity in $\mathscr{F}_\gamma(z)$. The question is whether or not there is a zero of $\rho - \boldsymbol{c}(1-\gamma/2-iz,-\gamma/2+iz)$ for some z with imaginary part smaller than $\gamma/2$. If there is, then this is the minimal pole. If not, then $i\gamma/2$ is the minimal pole. By Lemma 3, the zero in question is of the form z^*i for some positive real z^* satisfying $\rho - \boldsymbol{c}(1-\gamma/2+z^*,-\gamma/2-z^*) = 0$. If $z^* > \gamma/2$—in the subcritical case—the minimal pole for both integrals is at $i\gamma/2$, so

$$P/D \to \frac{\text{Res}\left\{\dfrac{e^{iuz}\mathscr{F}_\gamma(z)}{\rho - \boldsymbol{c}(1-\gamma/2-iz,-\gamma/2+iz)}; i\gamma/2\right\}}{\text{Res}\left\{e^{iuz}\mathscr{F}_\gamma(z); i\gamma/2\right\}} = \frac{1}{\rho - \boldsymbol{c}(1,-\gamma)}.$$

If $z^* < \gamma/2$—the supercritical case—the minimal pole is at iz^* for I_n and at $i\gamma/2$ for I_d, so

$$\begin{aligned} P/D &\to \frac{\text{Res}\left\{\dfrac{e^{iuz}\mathscr{F}_\gamma(z)}{\rho - \boldsymbol{c}(1-\gamma/2-iz,-\gamma/2+iz)}; iz^*\right\}}{\text{Res}\left\{e^{iuz}\mathscr{F}_\gamma(z); i\gamma/2\right\}} \\ &= e^{u(\gamma/2-z^*)} \cdot \frac{\text{Res}\left\{\dfrac{\mathscr{F}_\gamma(z)}{\rho - \boldsymbol{c}(1-\gamma/2-iz,-\gamma/2+iz)}; iz^*\right\}}{\text{Res}\left\{\mathscr{F}_\gamma(z); i\gamma/2\right\}} \\ &\to \infty\,. \end{aligned}$$

To see that the price-consumption ratio, $P/C = s \cdot P/D$, remains finite in this limit, we must evaluate $\lim_{s\to 0} s \cdot P/D$. Since $s = 1/(1+e^u) \sim e^{-u}$, we have, asymptotically,

$$P/C \to e^{u(\gamma/2 - z^* - 1)} \cdot \frac{\operatorname{Res}\left\{ \dfrac{\mathscr{F}_\gamma(z)}{\rho - \boldsymbol{c}(1-\gamma/2-iz, -\gamma/2+iz)}; iz^* \right\}}{\operatorname{Res}\left\{ \mathscr{F}_\gamma(z); i\gamma/2 \right\}},$$

which tends to zero as $u \to \infty$ because $\gamma/2 - z^* - 1 < 0$.

(ii) For the riskless rate, we seek the limit of

$$r = \frac{\displaystyle\int_{-\infty}^{\infty} \mathscr{F}_\gamma(z) e^{iuz} \cdot [\rho - \boldsymbol{c}(-\gamma/2 - iz, -\gamma/2 + iz)]\, dz}{\displaystyle\int_{-\infty}^{\infty} \mathscr{F}_\gamma(z) e^{iuz}\, dz}.$$

This is much simpler, because the minimal pole is $i\gamma/2$ for both numerator and denominator. It follows that $r \to \rho - \boldsymbol{c}(-\gamma/2 - i(i\gamma/2), -\gamma/2 + i(i\gamma/2)) = \rho - \boldsymbol{c}(0, -\gamma)$.

(iii) To calculate expected returns, we need the limiting expected capital gain (the first term on the right-hand side of (7)). This is asymptotically equivalent to

$$\frac{\displaystyle\int_{-\infty}^{\infty} \frac{e^{iuz}\mathscr{F}_\gamma(z)\boldsymbol{c}(1-\gamma/2-iz, \gamma/2+iz)}{\rho - \boldsymbol{c}(1-\gamma/2-iz, -\gamma/2+iz)}\, dz}{\displaystyle\int_{-\infty}^{\infty} \frac{e^{iuz}\mathscr{F}_\gamma(z)}{\rho - \boldsymbol{c}(1-\gamma/2-iz, -\gamma/2+iz)}\, dz} \equiv \frac{J_n}{J_d}$$

since the higher-order exponential terms e^{-mu} for $m \geq 1$ which appear in (7) become irrelevant exponentially fast as u tends to infinity. Again, there are two subcases. In the subcritical case, the minimal pole of each of J_n and J_d occurs at $i\gamma/2$, so

$$\lim_{u\to\infty} \mathbb{E}\, dP/P = \frac{\operatorname{Res}\left\{ \dfrac{e^{iuz}\mathscr{F}_\gamma(z)\boldsymbol{c}(1-\gamma/2-iz, \gamma/2+iz)}{\rho - \boldsymbol{c}(1-\gamma/2-iz, -\gamma/2+iz)}; i\gamma/2 \right\}}{\operatorname{Res}\left\{ \dfrac{e^{iuz}\mathscr{F}_\gamma(z)}{\rho - \boldsymbol{c}(1-\gamma/2-iz, -\gamma/2+iz)}; i\gamma/2 \right\}} = \boldsymbol{c}(1,0).$$

In the supercritical case, the minimal pole of each of J_n and J_d occurs at iz^*, so

$$\begin{aligned} \lim_{u\to\infty} \mathbb{E}\, dP/P &= \frac{\operatorname{Res}\left\{ \dfrac{e^{iuz}\mathscr{F}_\gamma(z)\boldsymbol{c}(1-\gamma/2-iz, \gamma/2+iz)}{\rho - \boldsymbol{c}(1-\gamma/2-iz, -\gamma/2+iz)}; iz^* \right\}}{\operatorname{Res}\left\{ \dfrac{e^{iuz}\mathscr{F}_\gamma(z)}{\rho - \boldsymbol{c}(1-\gamma/2-iz, -\gamma/2+iz)}; iz^* \right\}} \\ &= \boldsymbol{c}(1-\gamma/2+z^*, \gamma/2-z^*). \end{aligned}$$

Since instantaneous expected returns are the sum of expected capital gains and the dividend-price ratio, expected returns in the asymptotic limit are $\boldsymbol{c}(1,0)+\rho-\boldsymbol{c}(1,-\gamma)$ in the subcritical case, and $\boldsymbol{c}(1-\gamma/2+z^*,\gamma/2-z^*)$ in the supercritical case.

Subtracting the riskless rate, excess returns are $\boldsymbol{c}(1,0)+\boldsymbol{c}(0,-\gamma)-\boldsymbol{c}(1,-\gamma)$ in the subcritical case, and $\boldsymbol{c}(1-\gamma/2+z^*,\gamma/2-z^*)-\rho+\boldsymbol{c}(0,-\gamma)$ in the supercritical case. Since $\rho=\boldsymbol{c}(1-\gamma/2+z^*,-\gamma/2-z^*)$ by the definition of z^*, the excess return in the supercritical case can be rewritten as $\boldsymbol{c}(1-\gamma/2+z^*,\gamma/2-z^*)+\boldsymbol{c}(0,-\gamma)-\boldsymbol{c}(1-\gamma/2+z^*,-\gamma/2-z^*)$.

Step 3. If dividends are also independent across assets then we can decompose $\boldsymbol{c}(\theta_1,\theta_2)=\boldsymbol{c}_1(\theta_1)+\boldsymbol{c}_2(\theta_2)$ where $\boldsymbol{c}_i(\theta)\equiv\log\mathbb{E}\exp\theta y_{i1}$. It follows that in the subcritical case, $XS\to\boldsymbol{c}(1,0)+\boldsymbol{c}(0,-\gamma)-\boldsymbol{c}(1,-\gamma)=0$, and in the supercritical case,

$$\begin{aligned} XS &\to \boldsymbol{c}(1-\gamma/2+z^*,\gamma/2-z^*)+\boldsymbol{c}(0,-\gamma)-\boldsymbol{c}(1-\gamma/2+z^*,-\gamma/2-z^*) \\ &= \boldsymbol{c}_2(\gamma/2-z^*)+\boldsymbol{c}_2(-\gamma)-\boldsymbol{c}_2(-\gamma/2-z^*)\,. \end{aligned}$$

Step 4. This last expression is positive because $\boldsymbol{c}_2(x)$—as a CGF—is convex. To spell things out, $(\boldsymbol{c}_2(e)-\boldsymbol{c}_2(d))/(e-d)<(\boldsymbol{c}_2(g)-\boldsymbol{c}_2(f))/(g-f)$ whenever $d<e<f<g$. In the supercritical case, we have $-\gamma<-\gamma/2-z^*<0<\gamma/2-z^*$, so $[\boldsymbol{c}_2(-\gamma/2-z^*)-\boldsymbol{c}_2(-\gamma)]/[(-\gamma/2-z^*)-(-\gamma)]<[\boldsymbol{c}_2(\gamma/2-z^*)-\boldsymbol{c}_2(0)]/[(\gamma/2-z^*)-0]$ or equivalently, because $\boldsymbol{c}_2(0)=0$, $\boldsymbol{c}_2(-\gamma/2-z^*)-\boldsymbol{c}_2(-\gamma)<\boldsymbol{c}_2(\gamma/2-z^*)$, as required.

Step 5(i). Proof that $R_1<R_2$, assuming independence of dividends: In the subcritical case, $R_1=\rho+\boldsymbol{c}(1,0)-\boldsymbol{c}(1,-\gamma)$ and $R_2=\rho+\boldsymbol{c}(0,1)-\boldsymbol{c}(0,1-\gamma)$. Since we are assuming independence, we must show that $-\boldsymbol{c}_2(-\gamma)<\boldsymbol{c}_2(1)-\boldsymbol{c}_2(1-\gamma)$, or equivalently that $\boldsymbol{c}_2(1-\gamma)<\boldsymbol{c}_2(1)+\boldsymbol{c}_2(-\gamma)$, which follows by convexity of $\boldsymbol{c}_2(\cdot)$.

In the supercritical case, $R_1=\boldsymbol{c}(1-\gamma/2+z^*,\gamma/2-z^*)$ and $R_2=\boldsymbol{c}(1-\gamma/2+z^*,-\gamma/2-z^*)+\boldsymbol{c}(0,1)-\boldsymbol{c}(0,1-\gamma)$ (substituting in for ρ from the definition of z^*). By independence, it remains to show that $\boldsymbol{c}_2(\gamma/2-z^*)<\boldsymbol{c}_2(-\gamma/2-z^*)+\boldsymbol{c}_2(1)-\boldsymbol{c}_2(1-\gamma)$, or equivalently that $\boldsymbol{c}_2(1-\gamma)+\boldsymbol{c}_2(\gamma/2-z^*)<\boldsymbol{c}_2(1)+\boldsymbol{c}_2(-\gamma/2-z^*)$, which follows by convexity of $\boldsymbol{c}_2(\cdot)$.

Step 5(ii). Next, I show that in the supercritical case, $R_1\le G_1$ if $G_1\ge G_2$. We do not need the independence assumption here. Write $\theta=\gamma/2-z^*\in(0,1)$, so that the limiting $R_1=\boldsymbol{c}(1-\theta,\theta)$. The claim is that $\boldsymbol{c}(1-\theta,\theta)\le\boldsymbol{c}(1,0)$. This follows from the convexity of $\boldsymbol{c}(\cdot,\cdot)$, which implies that $\boldsymbol{c}(1-\theta,\theta)\le(1-\theta)\boldsymbol{c}(1,0)+\theta\boldsymbol{c}(0,1)$. By assumption, $\boldsymbol{c}(0,1)\le\boldsymbol{c}(1,0)$, so $\boldsymbol{c}(1-\theta,\theta)\le(1-\theta)\boldsymbol{c}(1,0)+\theta\boldsymbol{c}(1,0)=\boldsymbol{c}(1,0)$, as required.

Limiting quantities for the large asset. In the case of the large asset, the assumed finiteness of its price-dividend ratio excludes the possibility that the minimal pole lies below $(\gamma/2)i$. If we run through the above logic, the analogue of $\phi(z)$ is $\phi_2(z)\equiv\rho-\boldsymbol{c}(-\gamma/2+z,1-$

$\gamma/2 - z)$. But now we must have $\phi_2(\gamma/2) > 0$ by the finiteness condition. So the minimal pole must lie at $(\gamma/2)i$, and the result follows by calculating residues there, as above.

A.5.1 Asymptotics near the small-asset limit

To prove Proposition 7, we need to consider the *two* closest residues to the real axis. By assumption $z^* \in (\gamma/2-1, \gamma/2+1)$, so for price-dividend ratio and excess-return calculations, the closest residue is at $(\gamma/2)i$ and the next closest is at z^*i. For the riskless rate calculation, the two closest residues are at $(\gamma/2)i$ and $(\gamma/2+1)i$. The residues at $(\gamma/2)i$ were calculated in the previous section, so it only remains to compute the residues at z^*i and at $(\gamma/2+1)i$ for the integrands in question. In the case of the dividend yield, we must analyze

$$\begin{aligned}
\frac{D}{P} &= \frac{\displaystyle\int_{-\infty}^{\infty} e^{iuz}\mathscr{F}_\gamma(z)\,dz}{\displaystyle\int_{-\infty}^{\infty} \frac{e^{iuz}\mathscr{F}_\gamma(z)}{\rho - \boldsymbol{c}(1-\gamma/2-iz, -\gamma/2+iz)}\,dz} \\
&\doteq \frac{e^{-\gamma u/2}}{\dfrac{e^{-\gamma u/2}}{\rho - \boldsymbol{c}(1,-\gamma)} + \dfrac{\mathscr{B}(\gamma/2-z^*, \gamma/2+z^*)e^{-z^*u}}{\boldsymbol{c}_1(1-\gamma/2+z^*, -\gamma/2-z^*) - \boldsymbol{c}_2(1-\gamma/2+z^*, -\gamma/2-z^*)}},
\end{aligned}$$

where the second (approximate) equality follows by the residue theorem logic, as in the previous section, $\mathscr{B}(x,y) \equiv \Gamma(x)\Gamma(y)/\Gamma(x+y)$, and $\boldsymbol{c}_i(\cdot,\cdot)$ indicates the partial derivative of $\boldsymbol{c}(\cdot,\cdot)$ with respect to its ith argument.

In the subcritical case, $z^* > \gamma/2$, straightforward algebra gives

$$\frac{D}{P} \doteq \rho - \boldsymbol{c}(1,-\gamma) + \underbrace{\frac{-\mathscr{B}(\gamma/2-z^*, \gamma/2+z^*)\left[\rho - \boldsymbol{c}(1,-\gamma)\right]^2}{\boldsymbol{c}_1(1-\gamma/2+z^*, -\gamma/2-z^*) - \boldsymbol{c}_2(1-\gamma/2+z^*, -\gamma/2-z^*)}}_{B_2} e^{-u(z^*-\gamma/2)},$$

while in the supercritical case, $z^* < \gamma/2$, we have

$$\frac{D}{P} \doteq \underbrace{\frac{\boldsymbol{c}_1(1-\gamma/2+z^*, -\gamma/2-z^*) - \boldsymbol{c}_2(1-\gamma/2+z^*, -\gamma/2-z^*)}{\mathscr{B}(\gamma/2-z^*, \gamma/2+z^*)}}_{B_4} e^{-u(\gamma/2-z^*)}.$$

To see that $B_2 > 0$, note first that $\mathscr{B}(\gamma/2-z^*, \gamma/2+z^*)$ is negative: it equals $\Gamma(\gamma/2-z^*)\Gamma(\gamma/2+z^*)/\Gamma(\gamma)$, and $\Gamma(x)$ is negative for $x \in (-1,0)$ and positive for $x > 0$. Second, the denominator of B_2 is positive, because it has the opposite sign to the derivative of $\phi(z) \equiv \rho - \boldsymbol{c}(1-\gamma/2+z, -\gamma/2-z)$ with respect to z, evaluated at z^*. This derivative is negative because $\phi(z)$ is (i) concave in z (because $\boldsymbol{c}(\cdot,\cdot)$ is convex), (ii) positive at $z = 0$ by the first finiteness condition in Table 1, and (iii) zero at $z = z^*$ by the definition of z^*.

To see that $B_4 > 0$, the same logic shows that the numerator is positive. The denominator is also positive, because $\gamma/2 - z^* > 0$ so now $\mathscr{B}(\gamma/2 - z^*, \gamma/2 + z^*) > 0$. Similarly, $B_1 = \gamma\left[\boldsymbol{c}(1, -1-\gamma) - \boldsymbol{c}(0, -\gamma)\right]$, $B_3 = B_2\left[\rho - \boldsymbol{c}(1, -\gamma)\right] \cdot Y$, and $B_5 = \frac{B_4}{\rho - \boldsymbol{c}(1,-\gamma)} \cdot Y$, where

$$Y \equiv \left[\boldsymbol{c}(1,0) - \boldsymbol{c}(1,-\gamma) + \boldsymbol{c}(1-\gamma/2+z^*, -\gamma/2-z^*) - \boldsymbol{c}(1-\gamma/2+z^*, \gamma/2-z^*)\right].$$

It only remains to show that if the two assets have independent fundamentals, then $Y < 0$ in the supercritical case and $Y > 0$ in the nearly supercritical case. The former follows by the logic of Steps 3 and 4 of the previous subsection. The latter does too: the sign of the inequality is reversed because now $\gamma/2 < z^*$.

B The N-tree case

B.1 The expectation

To make a start, we seek the integral

$$I_N \equiv \int_{\mathbb{R}^{N-1}} \frac{e^{-ix_1z_1 - ix_2z_2 - \cdots - ix_{N-1}z_{N-1}}}{\left(e^{x_1/N} + \cdots + e^{x_{N-1}/N} + e^{-(x_1+x_2+\ldots+x_{N-1})/N}\right)^\gamma} \, dx_1 \, \ldots \, dx_{N-1} \, .$$

Write $x_N \equiv -x_1 - \cdots - x_{N-1}$ and, for $i = 1, \ldots, N$, define

$$t_i = \frac{e^{x_i/N}}{e^{x_1/N} + \cdots + e^{x_N/N}} \, . \tag{40}$$

The variables t_i range between 0 and 1, sum to 1, and satisfy $e^{x_i} = t_i^N / \prod_{k=1}^N t_k$. Since $t_N = 1 - t_1 - \cdots - t_{N-1}$, we can rewrite

$$x_i = N \log t_i - \sum_{k=1}^{N-1} \log t_k - \log\left(1 - \sum_{k=1}^{N-1} t_k\right), \quad i = 1, \ldots, N-1 \, . \tag{41}$$

To make the change of variables (40), we must calculate the Jacobian $J \equiv \left|\frac{\partial(x_1,\ldots,x_{N-1})}{\partial(t_1,\ldots,t_{N-1})}\right|$. From (41), $\frac{\partial x_i}{\partial t_j} = \frac{1}{t_N} - \frac{1}{t_j} + \frac{N\delta_{ij}}{t_i}$, where δ_{ij} equals one if $i = j$ and zero otherwise, so

$$\begin{aligned} \frac{\partial(x_1, \ldots, x_{N-1})}{\partial(t_1, \ldots, t_{N-1})} &= \begin{pmatrix} \frac{N}{t_1} & & & \\ & \frac{N}{t_2} & & \\ & & \ddots & \\ & & & \frac{N}{t_{N-1}} \end{pmatrix} + \begin{pmatrix} 1 \\ 1 \\ \vdots \\ 1 \end{pmatrix} \begin{pmatrix} \frac{1}{t_N} - \frac{1}{t_1} \\ \frac{1}{t_N} - \frac{1}{t_2} \\ \vdots \\ \frac{1}{t_N} - \frac{1}{t_{N-1}} \end{pmatrix}' \\ &\equiv \qquad \boldsymbol{A} \qquad + \qquad \boldsymbol{\alpha}\boldsymbol{\beta}' \, . \end{aligned}$$

The last line defines the $(N-1) \times (N-1)$ diagonal matrix $\boldsymbol{A}$ and the $(N-1)$-dimensional column vectors $\boldsymbol{\alpha}$ and $\boldsymbol{\beta}$. To calculate $J = \det\left(\boldsymbol{A} + \boldsymbol{\alpha}\boldsymbol{\beta}'\right)$ we can use

Fact 2 (Matrix determinant lemma)**.** *If $\boldsymbol{A}$ is an invertible matrix, and $\boldsymbol{\alpha}$ and $\boldsymbol{\beta}$ are column vectors of length equal to the dimension of $\boldsymbol{A}$, then* $\det\left(\boldsymbol{A}+\boldsymbol{\alpha}\boldsymbol{\beta}'\right)=\left(1+\boldsymbol{\beta}'\boldsymbol{A}^{-1}\boldsymbol{\alpha}\right)\det\boldsymbol{A}$.

In the present case, $\det\boldsymbol{A}=N^{N-1}/(t_1\cdots t_{N-1})$, and $\boldsymbol{A}^{-1}$ is diagonal with t_i/N as the ith entry along the diagonal. It follows that $J=N^{N-2}/(t_1\cdots t_N)$. Writing Π for the product $\prod_{k=1}^N t_k$ and making the substitution suggested in (40),

$$\begin{aligned} I_N &= \int \frac{\left(\frac{t_1^N}{\Pi}\right)^{-iz_1}\left(\frac{t_2^N}{\Pi}\right)^{-iz_2}\cdots\left(\frac{t_{N-1}^N}{\Pi}\right)^{-iz_{N-1}}}{\left(\frac{t_1+t_2+\cdots+t_N}{\Pi^{1/N}}\right)^{\gamma}}\cdot J\,dt_1\ldots dt_{N-1} \\ &= N^{N-2}\int\Big(t_1^{\gamma/N+iz_1+\cdots+iz_{N-1}-Niz_1}t_2^{\gamma/N+iz_1+\cdots+iz_{N-1}-Niz_2}\cdots \\ &\qquad \cdots t_{N-1}^{\gamma/N+iz_1+\cdots+iz_{N-1}-Niz_{N-1}}\cdot t_N^{\gamma/N+iz_1+\cdots+iz_{N-1}}\Big)\,\frac{dt_1\ldots dt_{N-1}}{t_1\ldots t_{N-1}t_N}\,. \end{aligned}$$

This is a Dirichlet surface integral with range of integration $[0,1]^{N-1}$. As shown in Andrews, Askey and Roy (1999, p. 34), it can be evaluated in terms of Γ-functions: we have

$$I_N=\frac{N^{N-2}}{\Gamma(\gamma)}\cdot\Gamma\left(\gamma/N+iz_1+iz_2+\ldots+iz_{N-1}\right)\cdot\prod_{k=1}^{N-1}\Gamma\left(\gamma/N+iz_1+\cdots+iz_{N-1}-Niz_k\right)\,.$$

Defining $\mathscr{G}_\gamma^N(\boldsymbol{z})=I_N/(2\pi)^{N-1}$, where $\boldsymbol{z}=(z_1,\ldots,z_{N-1})$, we have

$$\mathscr{G}_\gamma^N(\boldsymbol{z})=\frac{N^{N-2}}{(2\pi)^{N-1}}\cdot\frac{\Gamma\left(\gamma/N+iz_1+iz_2+\ldots+iz_{N-1}\right)}{\Gamma(\gamma)}\cdot\prod_{k=1}^{N-1}\Gamma\left(\gamma/N+iz_1+\cdots+iz_{N-1}-Niz_k\right)\,. \tag{42}$$

Writing $\boldsymbol{x}=(x_1,\ldots,x_{N-1})$, it follows from the Fourier inversion theorem that

$$\frac{1}{\left(e^{x_1/N}+e^{x_2/N}+\ldots+e^{-(x_1+x_2+\ldots+x_{N-1})/N}\right)^{\gamma}}=\int_{\mathbb{R}^{N-1}}\mathscr{G}_\gamma^N(\boldsymbol{z})e^{i\boldsymbol{z}'\boldsymbol{x}}\,d\boldsymbol{z}\,. \tag{43}$$

With $\boldsymbol{\alpha}\equiv(\alpha_1,\ldots,\alpha_N)'$ and $\widetilde{\boldsymbol{y}}_t\equiv(\widetilde{y}_{1t},\ldots,\widetilde{y}_{Nt})'$, we seek the expectation

$$E=\mathbb{E}\left[\frac{e^{\boldsymbol{\alpha}'\widetilde{\boldsymbol{y}}_t}}{\left(e^{y_{10}+\widetilde{y}_{1t}}+\cdots+e^{y_{N0}+\widetilde{y}_{Nt}}\right)^{\gamma}}\right].$$

Define the $(N-1)\times N$ matrix $\boldsymbol{Q}$ and vectors $\boldsymbol{q}_i$ by

$$\boldsymbol{Q}\equiv\begin{pmatrix}\boldsymbol{q}_2'\\ \boldsymbol{q}_3'\\ \vdots\\ \boldsymbol{q}_N'\end{pmatrix}\equiv\begin{pmatrix}-1 & N-1 & -1 & \cdots & -1\\ -1 & -1 & N-1 & \ddots & \vdots\\ \vdots & \vdots & \ddots & \ddots & -1\\ -1 & -1 & \cdots & -1 & N-1\end{pmatrix},$$

and let $\boldsymbol{q}_1 \equiv (N-1, \ldots, -1, -1)'$: this is the "missing" row that does *not* appear as the top row of $\boldsymbol{Q}$. Then, with $\boldsymbol{Q}(\boldsymbol{y}_0 + \widetilde{\boldsymbol{y}}_t)$ playing the role of $\boldsymbol{x}$ in expression (43),

$$\begin{aligned} E &= \mathbb{E}\left[\frac{e^{\boldsymbol{\alpha}'\widetilde{\boldsymbol{y}}_t - \boldsymbol{\gamma}'(\boldsymbol{y}_0+\widetilde{\boldsymbol{y}}_t)/N}}{\left(e^{\boldsymbol{q}_1'(\boldsymbol{y}_0+\widetilde{\boldsymbol{y}}_t)/N} + \cdots + e^{\boldsymbol{q}_N'(\boldsymbol{y}_0+\widetilde{\boldsymbol{y}}_t)/N}\right)^{\gamma}}\right] \\ &= e^{-\boldsymbol{\gamma}'\boldsymbol{y}_0/N}\int \mathscr{G}_\gamma^N(\boldsymbol{z}) e^{i\boldsymbol{z}'\boldsymbol{Q}\boldsymbol{y}_0} e^{\boldsymbol{c}(\boldsymbol{\alpha}-\boldsymbol{\gamma}/N+i\boldsymbol{Q}'\boldsymbol{z})t}\, d\boldsymbol{z}\,. \end{aligned} \tag{44}$$

B.2 Prices, expected returns, and interest rates

Using (44), the price-dividend ratio equals

$$\begin{aligned} P/D &= C_0^\gamma \int_0^\infty e^{-\rho t}\,\mathbb{E}\left[\frac{e^{\alpha_1\widetilde{y}_{1t}+\cdots+\alpha_N\widetilde{y}_{Nt}}}{\left(e^{y_{10}+\widetilde{y}_{1t}}+\cdots+e^{y_{N0}+\widetilde{y}_{Nt}}\right)^{\gamma}}\right] dt \\ &= C_0^\gamma \int_{t=0}^\infty e^{-\rho t}\left(e^{-\boldsymbol{\gamma}'\boldsymbol{y}_0/N}\int \mathscr{G}_\gamma^N(\boldsymbol{z}) e^{i\boldsymbol{z}'\boldsymbol{Q}\boldsymbol{y}_0} e^{\boldsymbol{c}(\boldsymbol{\alpha}-\boldsymbol{\gamma}/N+i\boldsymbol{Q}'\boldsymbol{z})t}\, d\boldsymbol{z}\right) dt \\ &= C_0^\gamma e^{-\boldsymbol{\gamma}'\boldsymbol{y}_0/N}\int \frac{\mathscr{G}_\gamma^N(\boldsymbol{z}) e^{i\boldsymbol{z}'\boldsymbol{Q}\boldsymbol{y}_0}}{\rho - \boldsymbol{c}(\boldsymbol{\alpha}-\boldsymbol{\gamma}/N+i\boldsymbol{Q}'\boldsymbol{z})}\, d\boldsymbol{z} \\ &= \left(e^{\boldsymbol{q}_1'\boldsymbol{y}_0/N}+\cdots+e^{\boldsymbol{q}_N'\boldsymbol{y}_0/N}\right)^{\gamma}\int \frac{\mathscr{G}_\gamma^N(\boldsymbol{z}) e^{i\boldsymbol{z}'\boldsymbol{Q}\boldsymbol{y}_0}}{\rho - \boldsymbol{c}(\boldsymbol{\alpha}-\boldsymbol{\gamma}/N+i\boldsymbol{Q}'\boldsymbol{z})}\, d\boldsymbol{z}\,. \end{aligned} \tag{45}$$

As in the two-asset case, I assume that $\mathrm{Re}\,[\rho - \boldsymbol{c}(\boldsymbol{\alpha}-\boldsymbol{\gamma}/N+i\boldsymbol{Q}'\boldsymbol{z})] > 0$ for all $\boldsymbol{z}$, which follows from the apparently weaker condition that $\rho - \boldsymbol{c}(\boldsymbol{\alpha}-\boldsymbol{\gamma}/N) > 0$.

To calculate expected capital gains, use (45) to write the price of the $\boldsymbol{\alpha}$-asset as

$$P = \sum_{\boldsymbol{m}} \binom{\gamma}{\boldsymbol{m}} \int \frac{\mathscr{G}_\gamma^N(\boldsymbol{z}) e^{(\boldsymbol{\alpha}-\boldsymbol{\gamma}/N+\boldsymbol{m}+i\boldsymbol{Q}'\boldsymbol{z})'\boldsymbol{y}_0}}{\rho - \boldsymbol{c}(\boldsymbol{\alpha}-\boldsymbol{\gamma}/N+i\boldsymbol{Q}'\boldsymbol{z})}\, d\boldsymbol{z}\,.$$

The sum is taken over all $\boldsymbol{m}$ whose entries are nonnegative integers which add up to γ. So,

$$\mathbb{E}\, dP = \sum_{\boldsymbol{m}} \binom{\gamma}{\boldsymbol{m}} \int \frac{\mathscr{G}_\gamma^N(\boldsymbol{z}) e^{(\boldsymbol{\alpha}-\boldsymbol{\gamma}/N+\boldsymbol{m}+i\boldsymbol{Q}'\boldsymbol{z})'\boldsymbol{y}_0}\boldsymbol{c}(\boldsymbol{\alpha}-\boldsymbol{\gamma}/N+\boldsymbol{m}+i\boldsymbol{Q}'\boldsymbol{z})}{\rho - \boldsymbol{c}(\boldsymbol{\alpha}-\boldsymbol{\gamma}/N+i\boldsymbol{Q}'\boldsymbol{z})}\, d\boldsymbol{z}\, dt\,,$$

whence

$$\begin{aligned} \Phi &= \sum_{\boldsymbol{m}} \binom{\gamma}{\boldsymbol{m}} \int \frac{\mathscr{G}_\gamma^N(\boldsymbol{z}) e^{(-\boldsymbol{\gamma}/N+\boldsymbol{m}+i\boldsymbol{Q}'\boldsymbol{z})'\boldsymbol{y}_0}\boldsymbol{c}(\boldsymbol{\alpha}-\boldsymbol{\gamma}/N+\boldsymbol{m}+i\boldsymbol{Q}'\boldsymbol{z})}{\rho - \boldsymbol{c}(\boldsymbol{\alpha}-\boldsymbol{\gamma}/N+i\boldsymbol{Q}'\boldsymbol{z})}\, d\boldsymbol{z} \\ &= \sum_{\boldsymbol{m}} \binom{\gamma}{\boldsymbol{m}} e^{m_1\boldsymbol{q}_1'\boldsymbol{y}_0/N+\cdots+m_N\boldsymbol{q}_N'\boldsymbol{y}_0/N} \int \frac{\mathscr{G}_\gamma^N(\boldsymbol{z}) e^{i\boldsymbol{z}'\boldsymbol{Q}\boldsymbol{y}_0}\boldsymbol{c}(\boldsymbol{\alpha}-\boldsymbol{\gamma}/N+\boldsymbol{m}+i\boldsymbol{Q}'\boldsymbol{z})}{\rho - \boldsymbol{c}(\boldsymbol{\alpha}-\boldsymbol{\gamma}/N+i\boldsymbol{Q}'\boldsymbol{z})}\, d\boldsymbol{z}\,. \end{aligned}$$

The price of a time-T zero-coupon bond is $B_T = \mathbb{E}\, e^{-\rho T}\left(\frac{C_T}{C_0}\right)^{-\gamma}$. Using (44),

$$\begin{aligned} B_T &= e^{-\rho T} C_0^\gamma\ \mathbb{E}\,\frac{1}{\left(e^{y_{10}+\widetilde{y}_{1T}}+\cdots+e^{y_{N0}+\widetilde{y}_{NT}}\right)^{\gamma}} \\ &= e^{-\rho T}\left(e^{\boldsymbol{q}_1'\boldsymbol{y}_0/N}+\cdots+e^{\boldsymbol{q}_N'\boldsymbol{y}_0/N}\right)^{\gamma}\int \mathscr{G}_\gamma^N(\boldsymbol{z}) e^{i\boldsymbol{z}'\boldsymbol{Q}\boldsymbol{y}_0} e^{\boldsymbol{c}(-\boldsymbol{\gamma}/N+i\boldsymbol{Q}'\boldsymbol{z})T}\, d\boldsymbol{z}, \end{aligned}$$

so the yield (from which the riskless rate follows by by l'Hôpital's rule) is

$$\mathscr{Y}(T) = \rho - \frac{1}{T}\log\left\{\left(e^{\boldsymbol{q}_1'\boldsymbol{y}_0/N} + \cdots + e^{\boldsymbol{q}_N'\boldsymbol{y}_0/N}\right)^{\gamma}\int \mathscr{G}_{\gamma}^{N}(\boldsymbol{z})e^{i\boldsymbol{z}'\boldsymbol{Q}\boldsymbol{y}_0}e^{\boldsymbol{c}(-\boldsymbol{\gamma}/N+i\boldsymbol{Q}'\boldsymbol{z})T}\,d\boldsymbol{z}\right\}.$$

B.3 A final change of variables

These expressions can be simplified by a final change of variables. Define $\widehat{\boldsymbol{z}} \equiv \boldsymbol{B}\boldsymbol{z}$, where

$$\boldsymbol{B} \equiv \begin{pmatrix} N-1 & -1 & \cdots & -1 \\ -1 & N-1 & \ddots & \vdots \\ \vdots & \ddots & \ddots & -1 \\ -1 & \cdots & -1 & N-1 \end{pmatrix}, \quad \text{so} \quad \boldsymbol{B}^{-1} = \frac{1}{N}\begin{pmatrix} 2 & 1 & \cdots & 1 \\ 1 & 2 & \ddots & \vdots \\ \vdots & \ddots & \ddots & 1 \\ 1 & \cdots & 1 & 2 \end{pmatrix}.$$

It follows that $\widehat{z}_k = Nz_k - z_1 - \cdots - z_{N-1}$, and that $\widehat{z}_1 + \cdots + \widehat{z}_{N-1} = z_1 + \cdots + z_{N-1}$. The Jacobian can be calculated using the matrix determinant lemma (Fact 2 above): $\det \boldsymbol{B}^{-1} = 1/N^{N-2}$, so—since $\boldsymbol{z} = \boldsymbol{B}^{-1}\widehat{\boldsymbol{z}}$—$d\boldsymbol{z}$ is replaced by $d\widehat{\boldsymbol{z}}/N^{N-2}$. Next, $\widehat{\boldsymbol{z}}$ was defined in such a way that $\mathscr{G}_{\gamma}^{N}(\boldsymbol{z})$, defined in equation (42), is equal to $N^{N-2}\mathscr{F}_{\gamma}^{N}(\widehat{\boldsymbol{z}})$, defined in the main text. Finally, noting that $\boldsymbol{B}^{-1}\boldsymbol{Q} = \boldsymbol{U}$ and $\boldsymbol{u} \equiv \boldsymbol{U}\boldsymbol{y}_0$, as defined in (22), we have $\boldsymbol{Q}'\boldsymbol{z} = \boldsymbol{Q}'\boldsymbol{B}^{-1}\widehat{\boldsymbol{z}} = \boldsymbol{U}'\widehat{\boldsymbol{z}}$ and $\boldsymbol{z}'\boldsymbol{Q}\boldsymbol{y}_0 = \widehat{\boldsymbol{z}}'\boldsymbol{U}\boldsymbol{y}_0 = \widehat{\boldsymbol{z}}'\boldsymbol{u} = \boldsymbol{u}'\widehat{\boldsymbol{z}}$. Proposition 8 follows after making these substitutions throughout the various integrals and dropping the hat on $\widehat{\boldsymbol{z}}$.